

DOE/PC/95251--T4

**SECOND GENERATION ADVANCED REBURNING  
FOR HIGH EFFICIENCY NO<sub>x</sub> CONTROL**

Progress Report No. 3 for Period  
April 1 - June 30, 1996

By:  
Vladimir M. Zamansky and Peter M. Maly  
Energy and Environmental Research Corporation  
18 Mason, Irvine, CA 92718

DOE Contract No. DE-AC22-95PC95251  
Phase I

Prepared for:  
William P. Barnett  
Project Manager  
U.S. Department of Energy  
Pittsburgh Energy Technology Center  
P.O. Box 10940, MS 922-316B  
Pittsburgh, PA 15236-0940

RECEIVED  
USDOE/PETC  
96 JUL 23 AM 11:14  
FEDERAL BUREAU OF INVESTIGATION  
U.S. DEPARTMENT OF JUSTICE

July 26, 1996

**MASTER**

*WJ*

**DISCLAIMER**

**Portions of this document may be illegible in electronic image products. Images are produced from the best available original document.**

## DISCLAIMER

This report was prepared as an account of work sponsored by an agency of the United States Government. Neither the United States Government nor any agency thereof, nor any of their employees, makes any warranty, express or implied, or assumes any legal liability or responsibility for the accuracy, completeness, or usefulness of any information, apparatus, product, or process disclosed, or represents that its use would not infringe privately owned rights. Reference herein to any specific commercial product, process, or service by trade name, trademark, manufacturer, or otherwise does not necessarily constitute or imply its endorsement, recommendation, or favoring by the United States Government or any agency thereof. The views and opinions of authors expressed herein do not necessarily state or reflect those of the United States Government or any agency thereof.

## TABLE OF CONTENTS

<u>Section</u>	<u>Page</u>
1.0 Introduction .....	1
2.0 Bench Scale Combustion Tests .....	4
2.1 Controlled Temperature Tower .....	4
2.2 Reburning Alone .....	6
2.3 Promoted SNCR Alone .....	8
2.4 Promoted AR - Lean .....	13
2.5 Promoted AR - Rich .....	18
2.6 Multiple Injection Advanced Reburning .....	23
2.7 Bench Scale Combustion Tests: Conclusions .....	23
3.0 Kinetics of Sodium Reactions .....	26
4.0 Kinetic Modeling .....	28
4.1 Injection of Ammonia Upstream of OFA .....	29
4.1.1 Effect of Oxygen .....	29
4.1.2 Effect of CO and H <sub>2</sub> .....	32
4.1.3 Effect of Initial NO Concentration .....	33
4.2 Injection of Ammonia with and after OFA .....	35
4.3 Burnout Zone Modeling: Conclusions .....	37
5.0 Future Plans .....	39
6.0 References .....	40

## LIST OF FIGURES

<u>Figure</u>	<u>Page</u>
Figure 1.1 SGAR schematic - definitions . . . . .	2
Figure 2.1.1. Controlled Temperature Tower (CTT) . . . . .	5
Figure 2.1.2. CTT temperature profiles . . . . .	7
Figure 2.2.1. NO reduction vs. CTT reburn heat input: no additives or promoters . . . . .	9
Figure 2.2.2. NO reduction vs. $SR_2$ for CTT gas reburn: no additives or promoters . . . . .	10
Figure 2.2.3. NO reduction vs. CTT reburn zone residence time: no additives or promoters	11
Figure 2.3.1. NO reduction vs. additive injection temperature for different N-agents . . . . .	12
Figure 2.3.2. NO reduction vs. additive injection for aqueous ammonia with promoters . . . . .	14
Figure 2.3.3. Comparison of promoted urea/OFA injection at CTT and BSF . . . . .	15
Figure 2.3.4. NO reduction vs. aqueous ammonia injection temperature for Delavan and Radial injectors . . . . .	16
Figure 2.4.1. Combined reburn/SNCR (AR-Lean) performance . . . . .	17
Figure 2.5.1. Combined reburn/SNCR (AR-Rich) performance . . . . .	19
Figure 2.5.2. NO control vs. Na promoter concentration . . . . .	20
Figure 2.5.3. NO reduction vs. initial NO concentration for rich side injection of $NH_4OH+Na_2CO_3$ . . . . .	21
Figure 2.5.4. NO reduction vs. additive $N/NO_x$ ratio for rich side injection of $NH_4OH$ and $Na_2CO_3$ . . . . .	22
Figure 2.6.1. MIAR: NO reduction vs. additive injection temperature reburn and both rich and lean side additives . . . . .	24
Figure 2.6.2. MIAR: NO reduction vs. additive injection temperature for reburn and both rich and lean side promoted additives. . . . .	25
Figure 4.1.1. Effect of $O_2$ co-injection with 500 ppm $NH_3$ into mixture I . . . . .	31
Figure 4.1.2. Effect of $SR_2$ on NO- $NH_3$ concentrations at 1300 K . . . . .	32
Figure 4.1.3. Temperature effect of $O_2$ co-injection with 200 ppm $NH_3$ . . . . .	34
Figure 4.1.4. Effect of NO initial level on resulting NO concentration . . . . .	35
Figure 4.2.1. Effect OFA co-injection with $NH_3$ on final NO concentration. $NSR_2 = 1.0$	37

## 1.0 Introduction

This project develops a family of novel NO<sub>x</sub> control technologies, Second Generation Advanced Reburning (SGAR), which has the potential to achieve 90+% NO<sub>x</sub> control at a significantly lower cost than selective catalytic reduction.

Phase I consists of six tasks:

- Task 1.1 Project Coordination and Reporting/Deliverables
- Task 1.2 Kinetics of Na<sub>2</sub>CO<sub>3</sub> Reactions with Flue Gas Components
- Task 1.3 20 kW Optimization Studies
- Task 1.4 20 kW Process Development Tests
- Task 1.5 Mechanism Development and Modeling
- Task 1.6 Design Methodology and Application

During the period (October 1, 1995 - March 31, 1996), the bench-scale facility, 20 kW Controlled Temperature Tower (CTT), was prepared for the experimental program (Task 1.3). Initial bench scale CTT experiments had been performed on different variants of the AR technology. A C-H-O-N chemical mechanism for description of the process chemistry (Task 1.5) was selected, and interaction of ammonia in the reburning zone was modeled. The effect of various additives on promotion of the NO-NH<sub>3</sub> interaction in the reburning zone was also evaluated.

This third reporting period (April 1 - June 30, 1996) included both experimental and modeling activities. Tests continued at the CTT, and the results have been reduced and are reported below. A study on high-temperature reactions of sodium promoters (Task 1.2) is underway at the University of Texas in Austin (UT). A brief literature review on high-temperature sodium reactions is included in this report. A high-temperature flow system with GC analysis was prepared at the University of Texas at Austin for the experimental program. Modeling focused on description of NO-NH<sub>3</sub> interaction in the burnout zone.

As in previous quarterly reports, Figure 1.1 summarizes the nomenclature used to refer to the

various regions of the Second Generation Advanced Reburning (SGAR) process. The region upstream of the reburning fuel injection is referred to as the "primary zone". The primary zone Stoichiometric Ratio ( $SR_1$ ) is maintained at  $SR_1=1.1$  for all tests and the initial NO concentration in this zone is referred to by a single subscript "i". The region between the reburning fuel and overfire air (OFA) injection is referred to as the "reburning zone". The reburning fuel is injected at a temperature of  $T_1$ . The first N-agent ( $A_1$ ) is introduced at  $T_2$  with a Nitrogen Stoichiometric

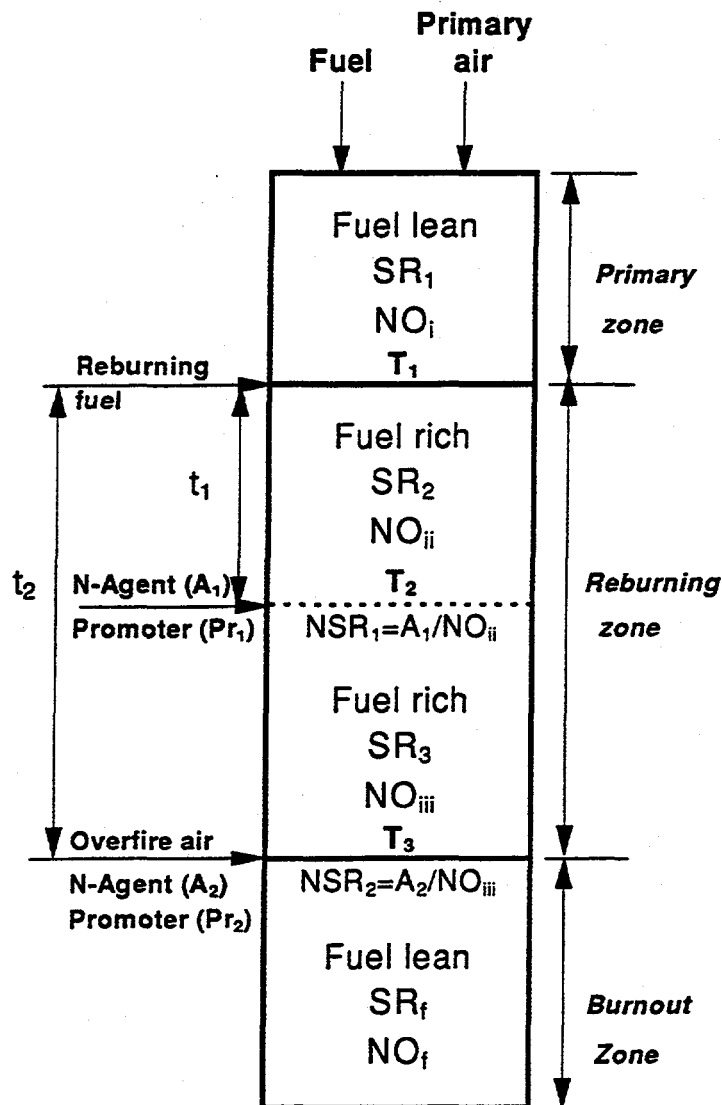


Figure 1.1 SGAR schematic - definitions.

molar Ratio  $NSR_1 = A_1 / NO_{ii}$  into the reburn zone. This zone is divided into two fuel rich zones

with stoichiometries  $SR_2$  and  $SR_3$ . NO concentration upstream of the first N-agent injection is referred to as "ii". NO reduction from  $NO_i$  to  $NO_{ii}$  is caused by reburning only. The first N-agent is injected with or without promoters ( $Pr_1$ ) with a  $t_1$  delay time after RF injection. NO concentration downstream of the  $A_1$  injection is called  $NO_{iii}$ , and NO reduction from  $NO_{ii}$  to  $NO_{iii}$  is caused by the first N-agent. Overfire air is injected at  $T_3$  with a  $t_2$  delay time after RF injection. OFA is the carrier gas for injecting the second N-agent ( $A_2$ ), which is injected with or without promoters ( $Pr_2$ ).  $A_2$  is injected with  $NSR_2=A_2/NO_{iii}$ . The downstream region is referred to as the "burnout zone". Stoichiometric ratio in this zone is  $SR_f$ , and the final NO concentration is  $NO_f$ .



## 2.0 Bench Scale Combustion Tests

The Second Generation Advanced Reburning (SGAR) process includes various combinations of reburning, nitrogen agent injection into the reburn zone, nitrogen agent injection downstream of the reburn zone, and promoter injection. Tests were conducted at EER's Controlled Temperature Tower (CTT) to optimize each component of the technology individually and then to optimize overall performance of the combined process. Several nitrogen agents were tested. Sodium was used as the main promoter because its performance has been successfully demonstrated in the past. Specific test series included:

- Reburning alone
- Promoted SNCR alone
- Promoted advanced reburning (lean and rich)
- Multiple injection advanced reburning

All tests were conducted in the CTT with natural gas firing at 20 kW. The test facility and results of each test series are described below.

### 2.1 Controlled Temperature Tower

As shown in Figure 2.1.1, the CTT is a refractory lined, vertically down-fired combustion test facility designed to provide precise control of furnace temperature and gas composition. It consists of a variable swirl diffusion burner and a refractory furnace which is equipped with backfired heating channels. The furnace has an inside diameter of 20 cm and a total height of 4 m. The backfired channels are designed to provide external heating to the refractory walls, allowing the rate of temperature decay to be controlled. Because of the relatively small size of the CTT, it is possible to use bottled gases (e.g. O<sub>2</sub>, N<sub>2</sub>, SO<sub>2</sub>) to control furnace gas composition. In addition, characteristic mixing times in the CTT furnace are on the order of 100 ms, making it straightforward to separate zones and characterize individual processes.

Specific test equipment for the SGAR tests included injectors for the reburn fuel, N-

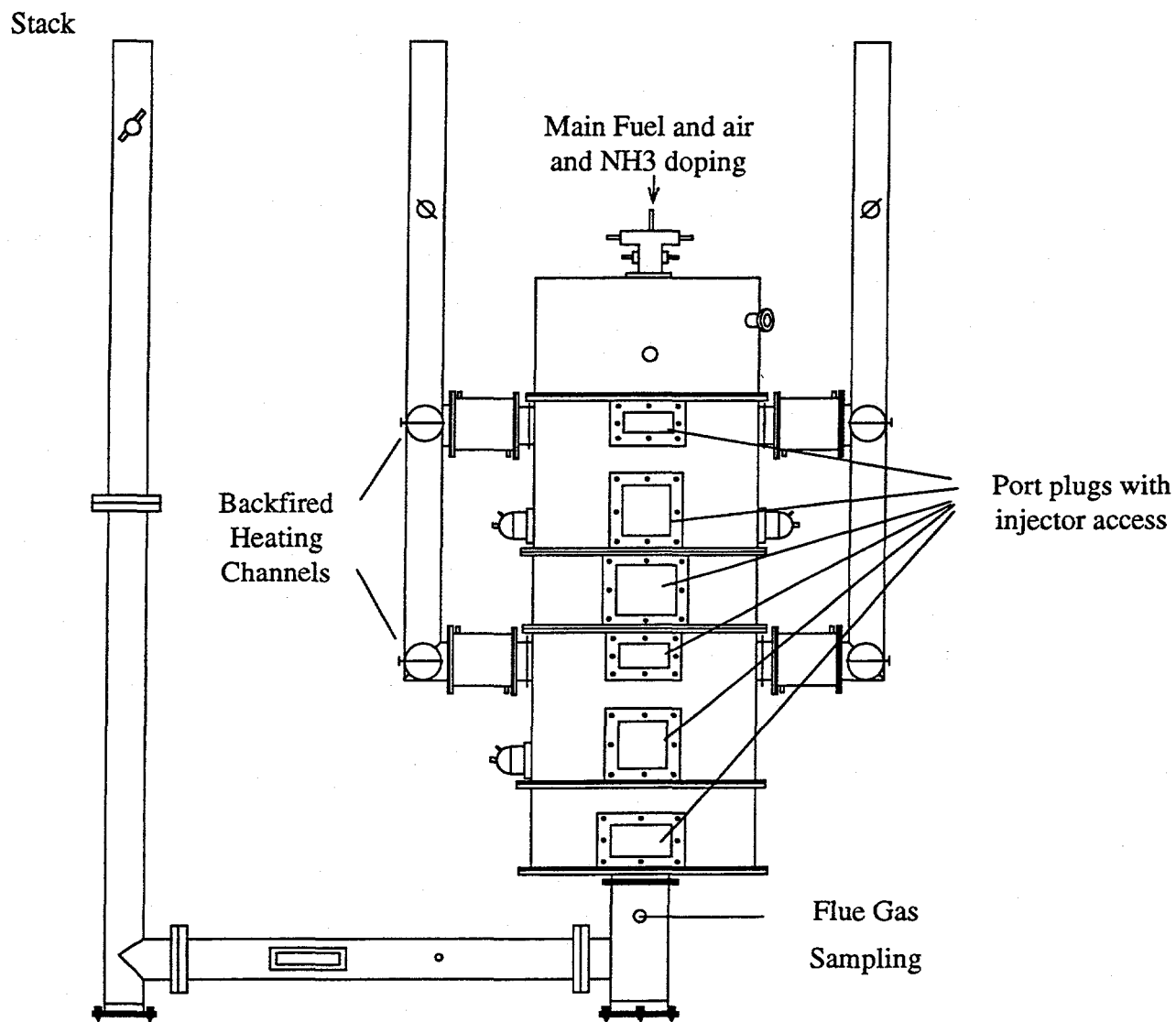


Figure 2.1.1. Controlled Temperature Tower (CTT)

agent/promoters, and overfire air. The reburn fuel and overfire air were injected through radial injectors aligned upwards, i.e. countercurrent to the gas flow. The N-agents and promoters were injected through axial injectors aligned downwards. Delavan twin fluid nozzles were used for additive atomization, with bottled nitrogen as the atomization medium. Prior to the experiments, system temperature profiles were measured under various test configurations using a suction pyrometer. These profiles are presented in Figure 2.1.2.

Proper operation of system instrumentation was verified before the tests began, including thermocouples, pressure gauges, and the flue gas sample system. A continuous emissions monitoring system (CEMS) was used for on-line analysis of flue gas composition. The CEMS consisted of a heated sample line, sample conditioning system (to remove moisture and particulate), and gas analyzers. Species analyzed, detection principles, and detection limits were as follows:

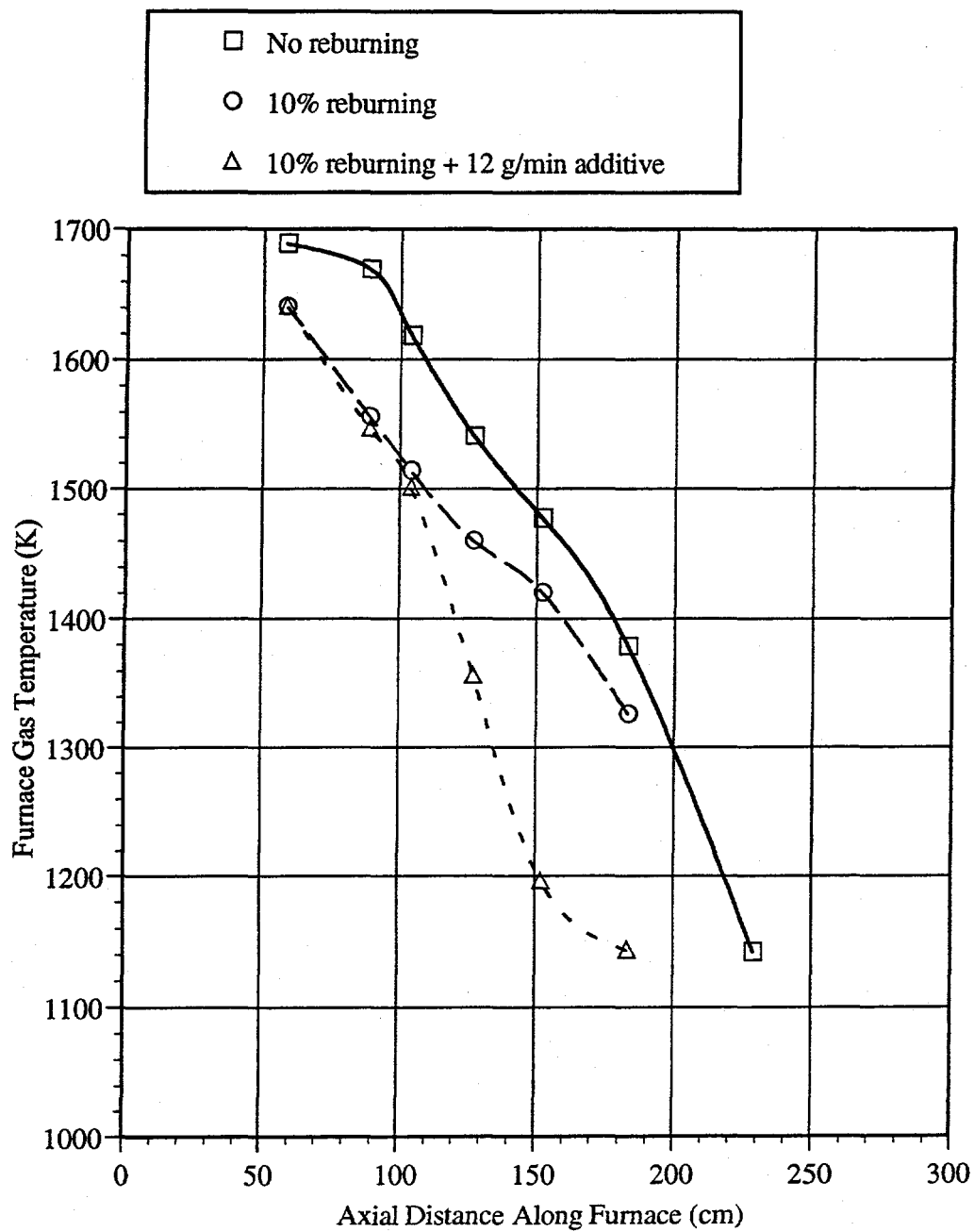
- O<sub>2</sub>: paramagnetism, 0.1%
- NO<sub>x</sub>: chemiluminescence, 1 ppm
- CO: nondispersive infrared, 1 ppm
- CO<sub>2</sub>: nondispersive infrared, 0.1%
- N<sub>2</sub>O: nondispersive infrared, 1 ppm

Certified zero and span gases were used to calibrate the analyzers. A chart recorder was used to provide a hard copy of analyzer outputs.

## 2.2 Reburning Alone

The first series of tests was designed to define the nominal performance of gas reburning without any additives. Test variables included reburn heat input (i.e. SR<sub>2</sub>), reburn zone residence time, and reburn fuel transport medium (air or nitrogen). Baseline conditions were as follows:

- Reburn fuel injection temperature = 1670 K
- SR<sub>1</sub>=1.10



Main burner: natural gas firing @ 20kW

Figure 2.1.2. CTT Temperature Profiles

- $SR_3=1.15$
- Overfire air injection temperature = 1530 K
- Reburn zone residence time = 350 msec
- $NO_i = 600$  ppm as measured

Figure 2.2.1 shows the impact of varying reburn fuel heat input upon NO reduction. For both air and nitrogen transport, performance increased with increasing reburn heat input. Maximum NO reductions were 42% and 59% with air and nitrogen transport, respectively. On the basis of reburn heat input nitrogen transport gave greater NO reduction than air transport. However, this is primarily because nitrogen transport gives lower reburn zone stoichiometry than air. As shown in Figure 2.2.2, when results are compared on the basis of  $SR_2$ , nitrogen and air transport data are nearly identical.

Reburn zone residence time was varied by moving the overfire air injector to different axial furnace positions. Reburn zone residence time was varied from 200 to 1600 msec at 10% reburn heat input. This corresponds to an overfire air injection temperature range of 1140 to 2190 K. As shown in Figure 2.2.3, with nitrogen transport NO control increased from 35 to 58% as reburn zone residence time increased from 200 to 1600 msec. With air transport NO control was not dependent upon residence time.

### 2.3 Promoted SNCR Alone

Tests were then conducted to optimize performance of SNCR additives and promoters without reburning. Test variables included additive type, additive injection temperature, and promoter type. Figure 2.3.1 compares performance of ammonia gas, urea, and ammonium sulfate with and without sodium carbonate promoter. Optimum injection temperature for each of the three unpromoted additives was approximately 1390 K, which is several hundred degrees hotter than the conventional optimum. This is attributed to the injector configuration, in which the additive was injected axially through a Delavan twin fluid nozzle in the same direction as the furnace gas flow. Because of the axial injection and droplet evaporation time, the true temperature seen by the additives was likely lower than the measured furnace temperature. Ammonia gas and urea

Main Fuel: Natural gas @ 20 kW  
Reburn fuel: Natural gas  
Reburn T=1670K  
SR1=1.10  
OFA T= 1530K  
Reburn zone residence time = 0.35 sec  
NOi=600 ppm as meas

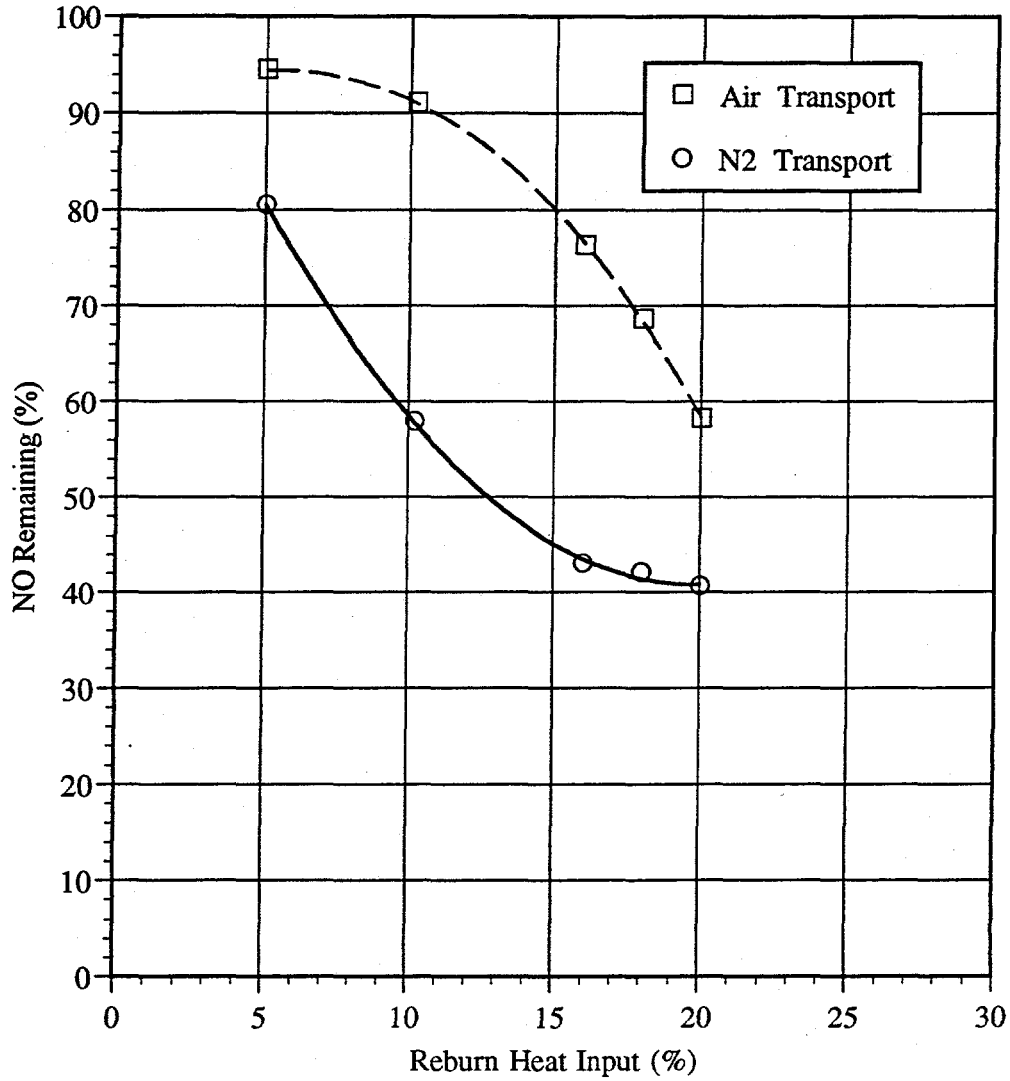


Figure 2.2.1. NO reduction vs. reburn heat input for CTT gas reburn: No additives or promoters

Main Fuel: Natural gas @ 20 kW  
Reburn fuel: Natural gas  
Reburn T=1670 K  
SR1=1.10  
OFA T= 1530 K  
Reburn zone residence time = 0.35 sec  
NOi=600 ppm as meas

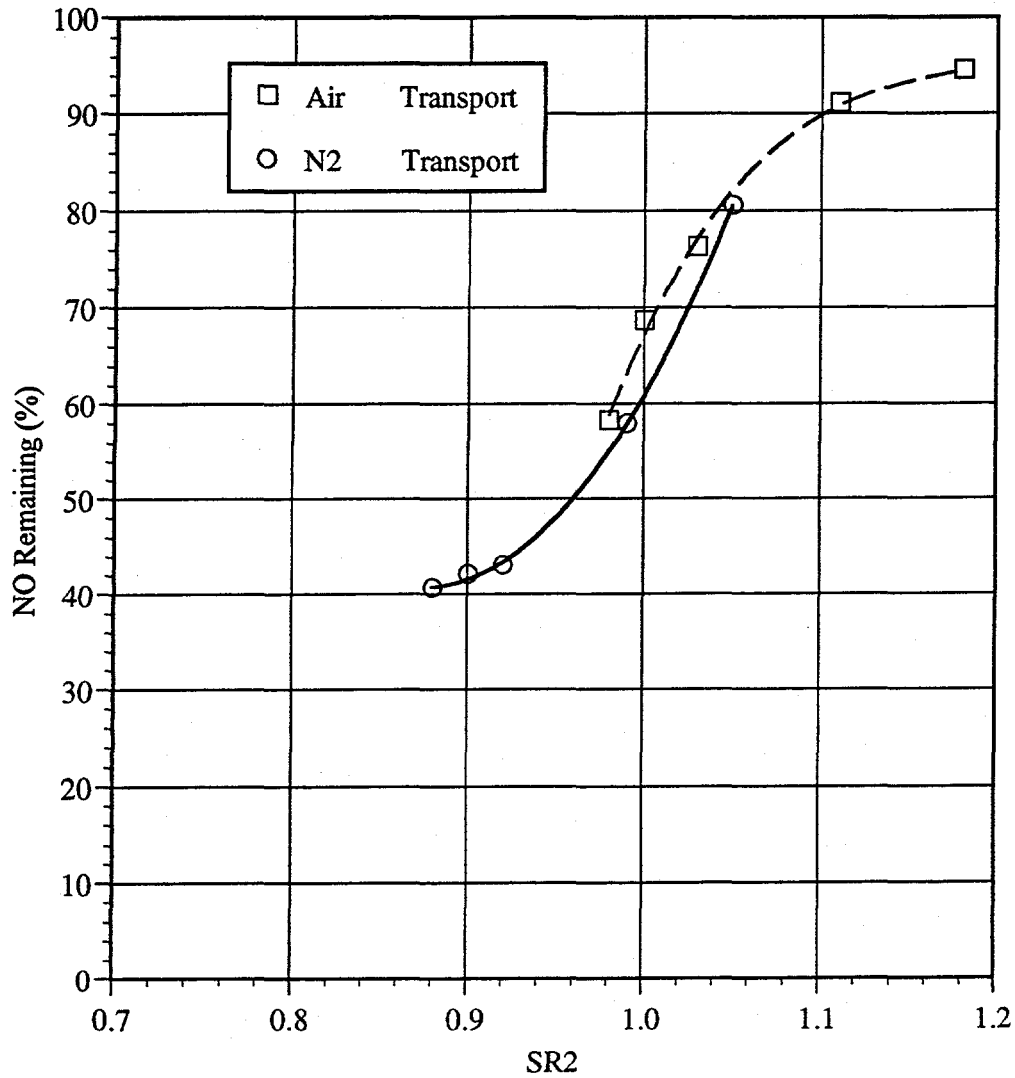


Figure 2.2.2. NO reduction vs. SR2 for CTT gas reburn: No additives or promoters

Main Fuel: Natural gas @ 20 kW  
Reburn fuel: Natural gas  
Reburn T=1670 K  
SR1=1.10  
10.2% Reburn  
SR2 (air)=1.10, SR2(N2)=0.99  
OFA T: varied  
NOi=600 ppm as meas

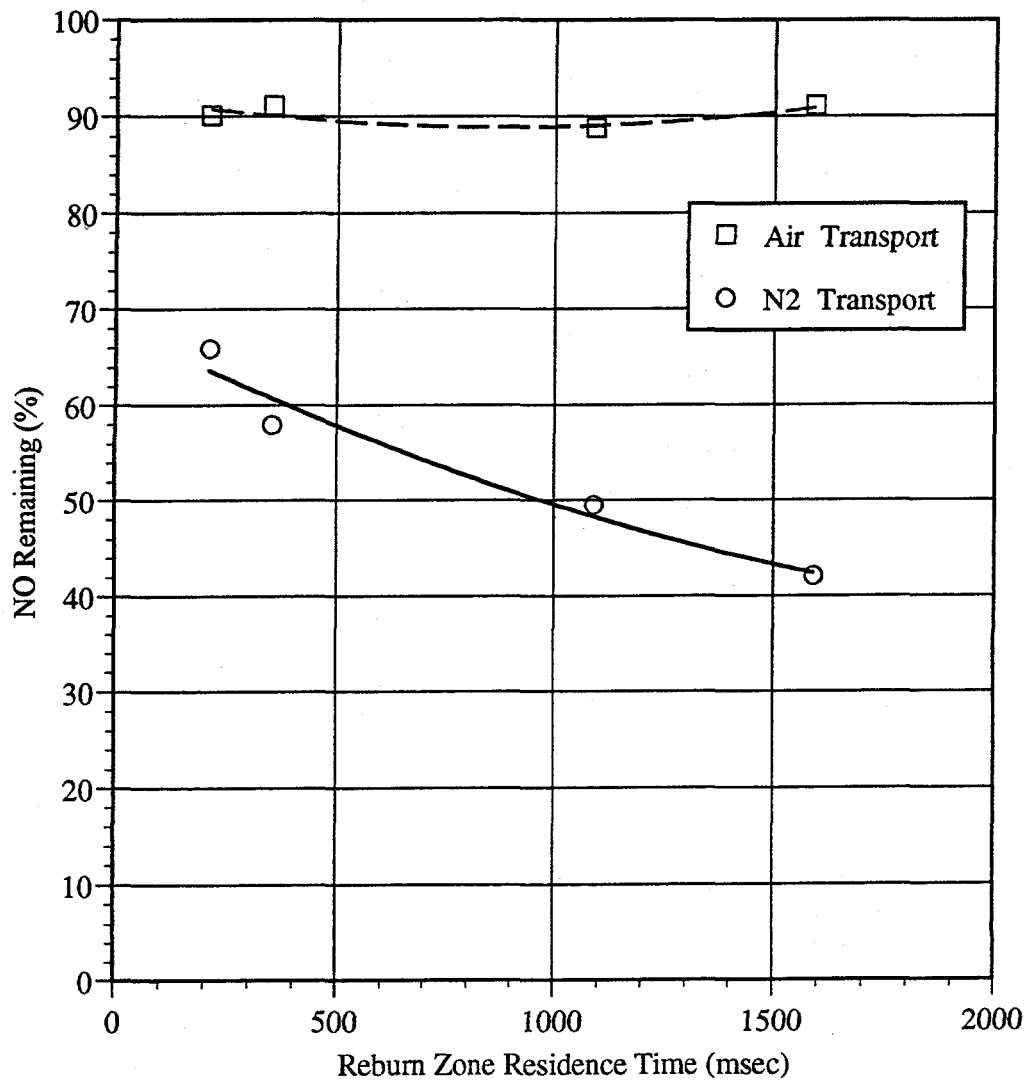


Figure 2.2.3. NO reduction vs. reburn zone residence time for gas reburn: No additives or promoters



Main Fuel: Natural gas @ 20 kW  
 No Return  
 SR1=1.15  
 NO<sub>i</sub>=300 ppm as meas  
 N/NO<sub>i</sub>=1.5

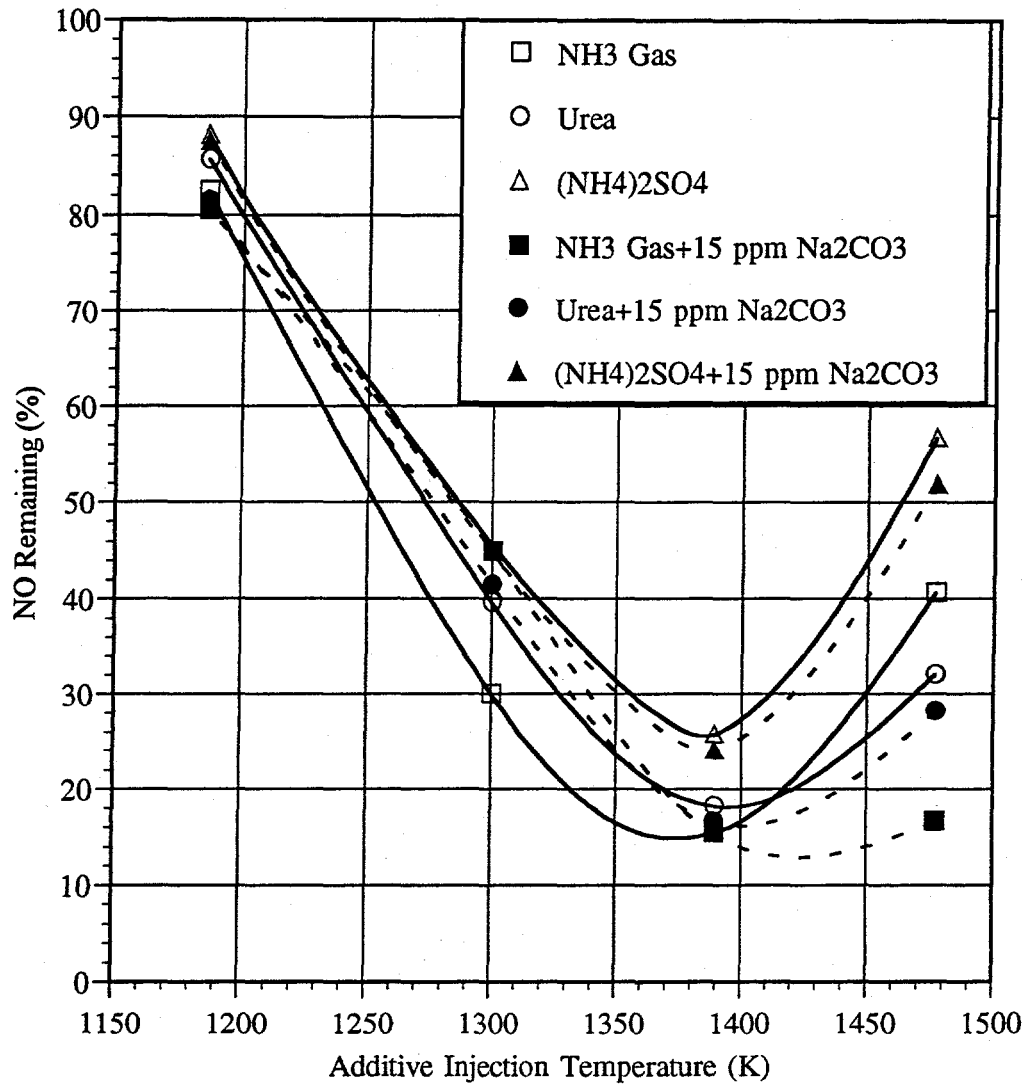


Figure 2.3.1. NO reduction vs. additive injection temperature for different N-agents

both performed somewhat better than ammonium sulfate. Sodium carbonate promoter had a slightly beneficial effect which was most noticeable at higher injection temperatures.

Sodium promoters tested included sodium carbonate, sodium bicarbonate, and sodium hydroxide. Figure 2.3.2 shows the impact of these promoters upon aqueous ammonia performance. Each compound was injected to provide 30 ppm sodium in the flue gas. The promoters shifted the optimum injection temperature to the right but did not appear to increase maximum NO reduction. This would appear to contradict earlier results indicating that sodium widened the optimum temperature window, shifted it to the left (i.e. to cooler temperatures), and increased maximum NO reduction. The earlier tests were conducted at EER's Boiler Simulator Furnace (BSF) at 200 kW, using a radial injector aligned countercurrent to the furnace gas flow. One day of testing was performed at the BSF to verify the previous results. As shown in Figure 2.3.3 the promoter was significantly more effective at the BSF than at the CTT. Other than the difference in scale, the main difference between the two test systems was that a radial injector was used at the BSF and an axial injector was used at the CTT. Therefore, a radial injector was fabricated and tested at the CTT. As shown in Figure 2.3.4, optimum injection temperature with the radial nozzle was 60 K lower than that with the axial injector with the Delavan nozzle. However, the promoter still had a minimal effect with the radial injector. It is believed that the difference between the CTT and BSF results lies in differences between the atomizer configurations, mixing, and droplet evaporation times. Specifically, the water-cooled injector used to inject the N-agents alters furnace gas temperatures, thus impacting performance. Thus, the sodium performance at low injection temperatures is expected to be better at higher scale where the cold injector does not significantly affect the flue gas temperature.

#### **2.4 Promoted AR - Lean**

In the next set of tests, reburning was coupled with the injection of a single nitrogen agent, both with and without promoters. N-agent was injected with the overfire air. Reburn heat input was 10%. Figure 2.4.1 shows results obtained with the nitrogen agent injected with the overfire air. The overfire air injection temperature was varied. This changed the reburn zone residence time, causing reburn performance to vary. Aqueous ammonia, urea, and ammonium sulfate were tested,

Main Fuel: Natural gas @ 20 kW  
No Reburn  
SR1=1.15  
NOi=300 ppm as meas  
N/NOi=1.5

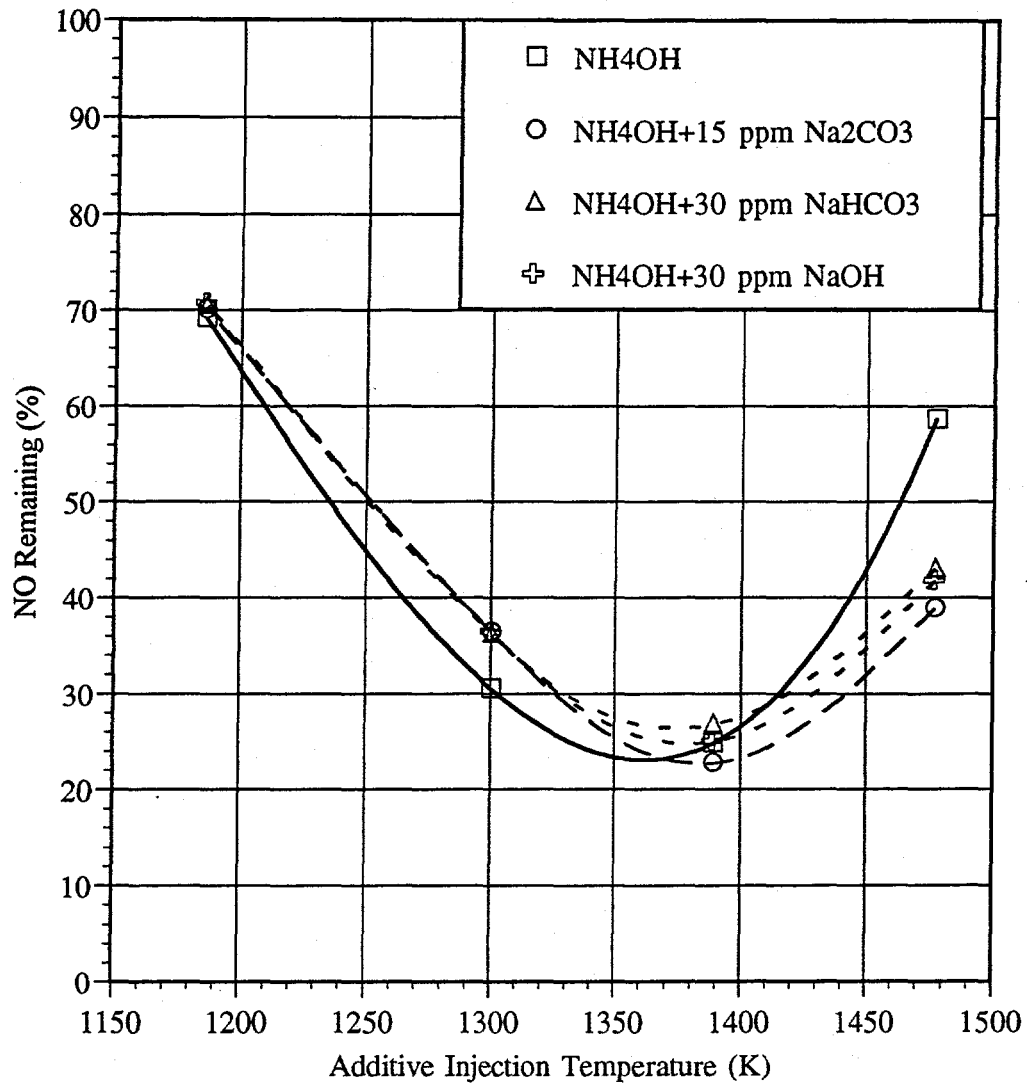


Figure 2.3.2. NO reduction vs. additive injection temperature for aqueous ammonia with promoters

Main Fuel: Natural gas  
 No Return, SR1=1.15  
 NO<sub>i</sub>=300 ppm as meas  
 N/NO<sub>i</sub>=1.5

CTT Firing rate: 20 kW  
 BSF Firing rate: 200 kW  
 CTT nozzle: axial, aligned downwards  
 BSF nozzle: radial, aligned upwards

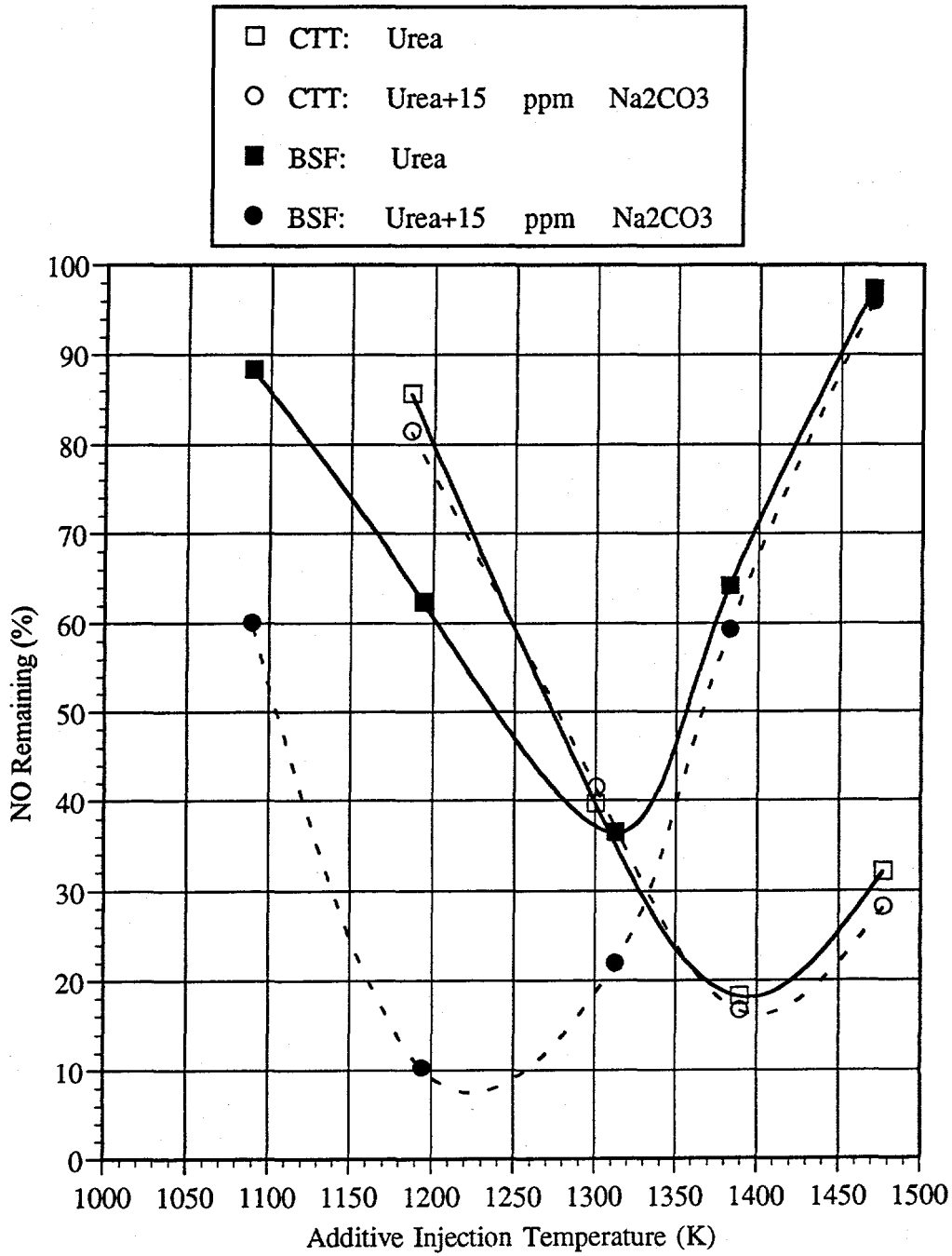


Figure 2.3.3. Comparison of promoted urea/OFA injection at CTT and BSF.

Main Fuel: Natural gas @ 20 kW  
No Return  
SR1=1.15  
NO<sub>i</sub>=300 ppm as meas  
N/NO<sub>i</sub>=1.5

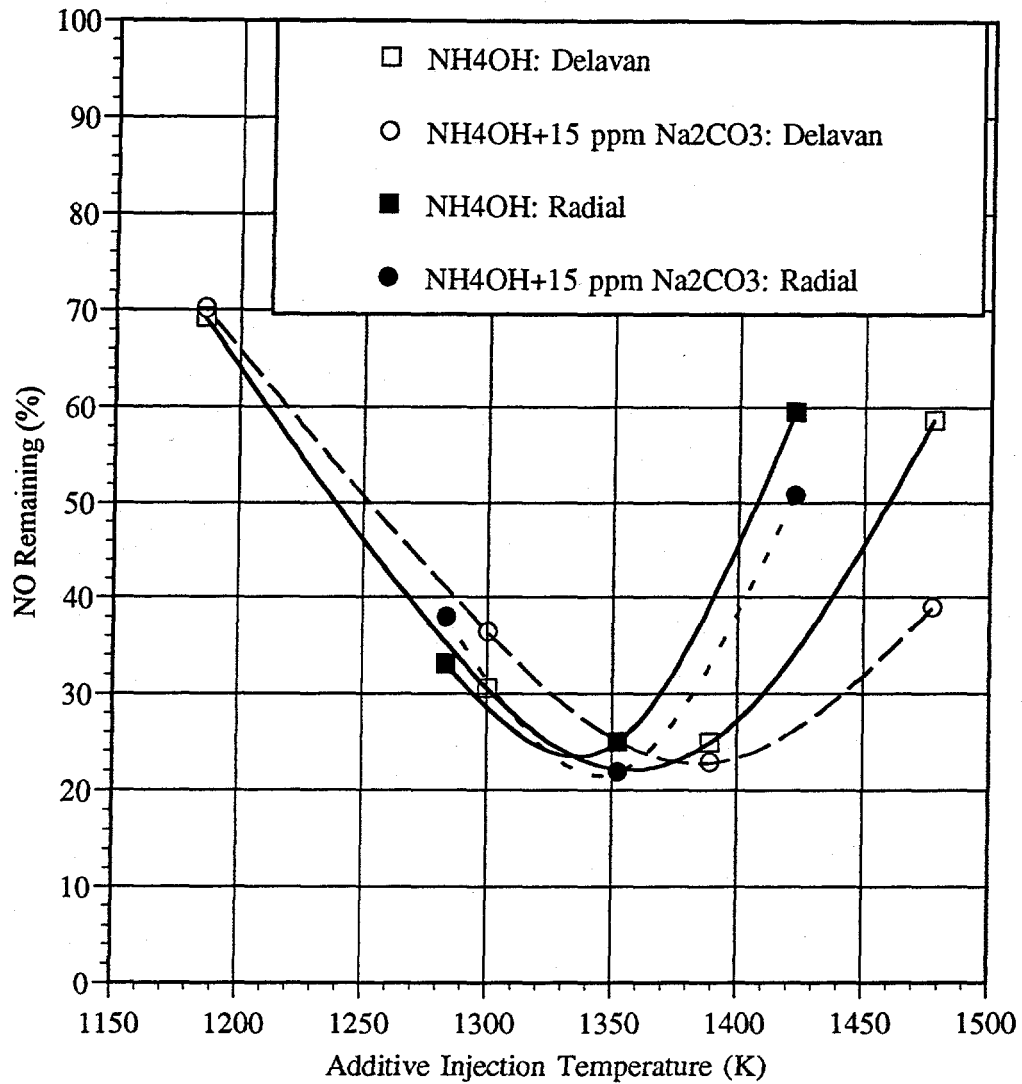


Figure 2.3.4. NO reduction vs. aqueous ammonia injection temperature for Delavan and Radial injectors.

Main Fuel: Natural gas @20 kW  
 10% Reburn @ 1670 K, N2 transport  
 Reburn zone res. time varies  
 SR1=1.10, SR2=0.99, SR3=1.15  
 NOi=600 ppm as meas  
 N/NOii=1.5  
 N agent added with OFA

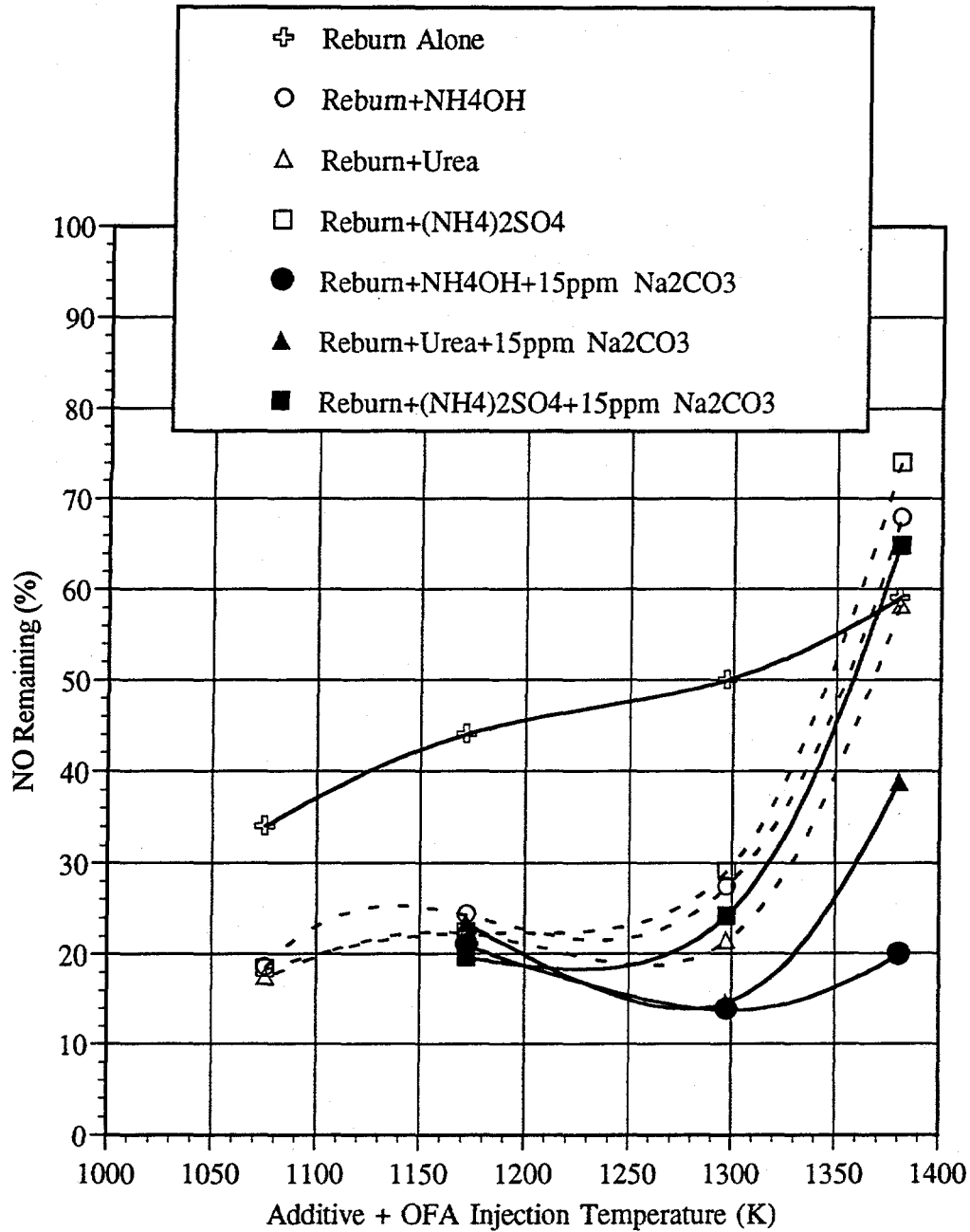


Figure 2.4.1 Combined reburn/SNCR (AR lean) performance.

each both with and without 15 ppm of sodium carbonate promoter. The listed promoter concentration assumes complete conversion to the gas phase. Aqueous ammonia and urea performed somewhat better than ammonium sulfate. Sodium carbonate both expanded the optimum temperature window to the right (i.e. to higher temperatures) and increased maximum NO control. The highest NO reduction achieved was 87% with both promoted aqueous ammonia and promoted urea at an injection temperature of 1290 K.

## 2.5 Promoted AR - Rich

In the next tests aqueous ammonia and urea were injected into the fuel rich reburn zone. Overfire air was added at 1160 K. As shown in Figure 2.5.1, the impact of the promoter was pronounced for this test system. Sodium carbonate shifted the optimum temperature to the right and significantly widened the temperature window. Maximum NO reduction was 88%, obtained with both promoted aqueous ammonia and promoted urea at an injection temperature of 1450 K.

Parametric studies were then conducted to evaluate the impact of three process variables: sodium concentration, initial NO concentration, and N-agent to NO stoichiometric ratio. Sodium concentration was varied during injection of aqueous ammonia and urea into the fuel rich zone with 10% reburning. As shown in Figure 2.5.2, NO control increased as Na concentration increased from 0 to 30 ppm, and then levelled off as [Na] was further increased to over 100 ppm. Even 10 ppm Na (i.e. 5 ppm  $\text{Na}_2\text{CO}_3$ ) reduced the remaining NO fraction by 21 percentage points, from 42 to 21%.

Initial NO concentration was varied from 150 to 950 ppm during tests with reburn alone and reburn plus injection of aqueous ammonia and sodium carbonate. As shown in Figure 2.5.3, NO reduction increased with increasing  $\text{NO}_i$ . For reburn plus injection of aqueous ammonia and sodium carbonate over 90% NO control was obtained at  $\text{NO}_i=950$  ppm.

Nitrogen agent to  $\text{NO}_i$  stoichiometric ratio was then varied from 0 to 2.0. As shown in Figure 2.5.4, NO reduction increased with increasing N-agent stoichiometric ratio. NO reduction was 93% at a stoichiometric ratio of 2.0.

Main Fuel: Natural gas @20 kW  
 10% Reburn @ 1670 K, N2 transport  
 Reburn zone res. time=0.72 sec  
 OFA added at 1160 K  
 SR1=1.10, SR2=0.99, SR3=1.15  
 NO<sub>i</sub>=600 ppm as meas  
 N/NO<sub>ii</sub>=1.5  
 N agent added in reburn zone

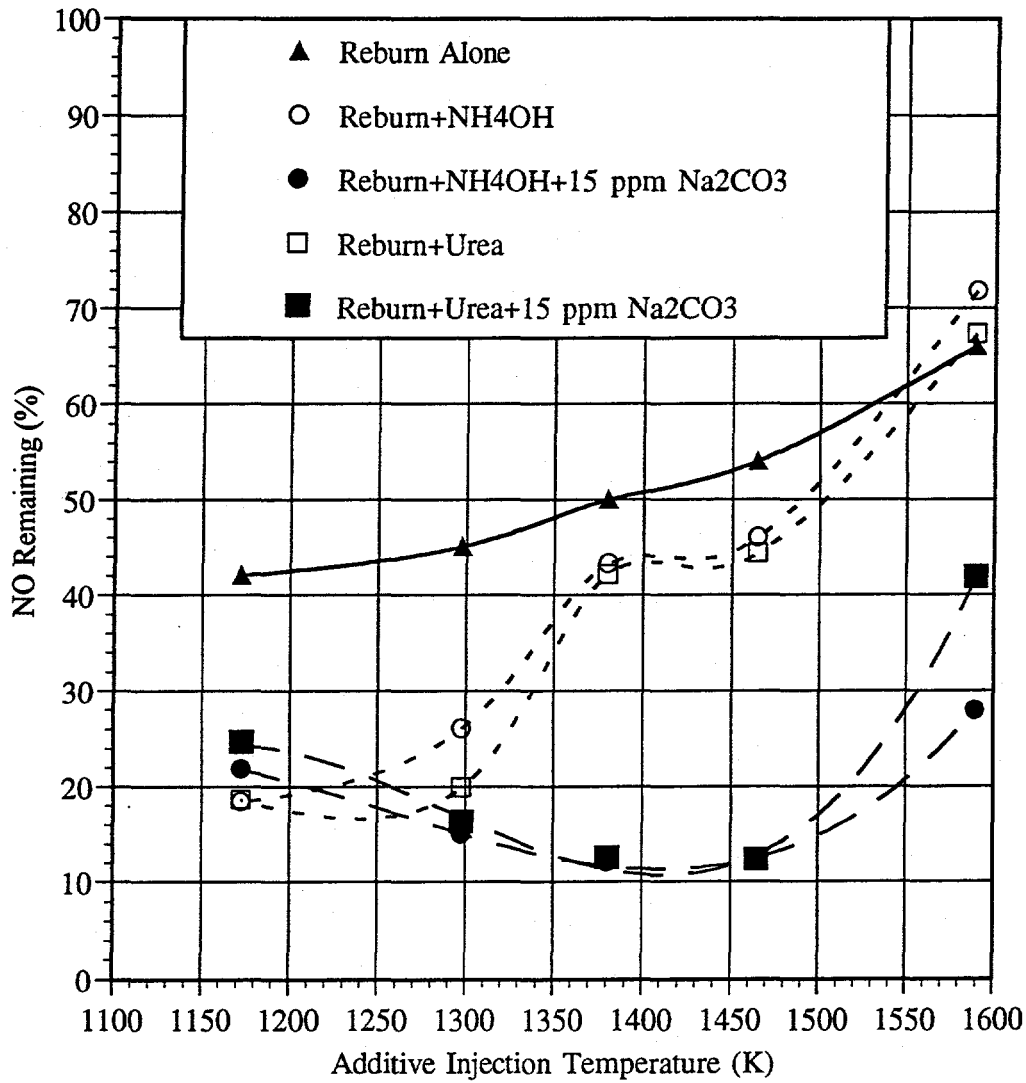


Figure 2.5.1. Combined reburn/SNCR (AR-Rich) performance.



Main Fuel: Natural gas @ 20 kW  
10% Reburn @ 1670 K, N<sub>2</sub> transport  
Reburn zone res. time=0.72 sec  
OFA added at 1160 K  
SR1=1.10, SR2=0.99, SR3=1.15  
NO<sub>i</sub>=600 ppm as meas  
N/NO<sub>ii</sub>=1.5  
Injection Temp=1380 K

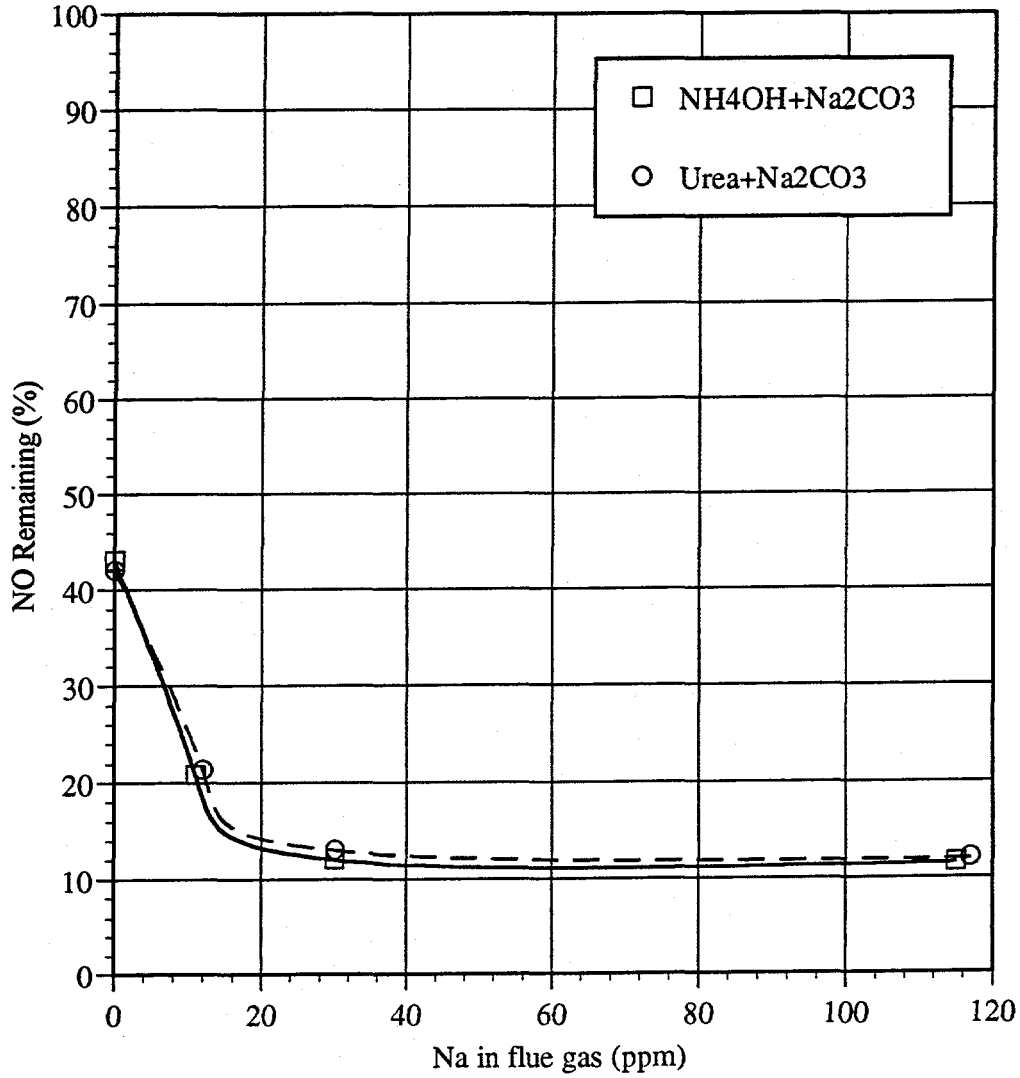


Figure 2.5.2. NO control vs. Na promoter concentration

Main Fuel: Natural gas @ 20 kW  
10% Reburn @ 1670 K  
OFA @ 1300 K  
Additive @ 1460 K  
SR1=1.10, SR2=0.99, SR3=1.15  
N/NOi=1.5

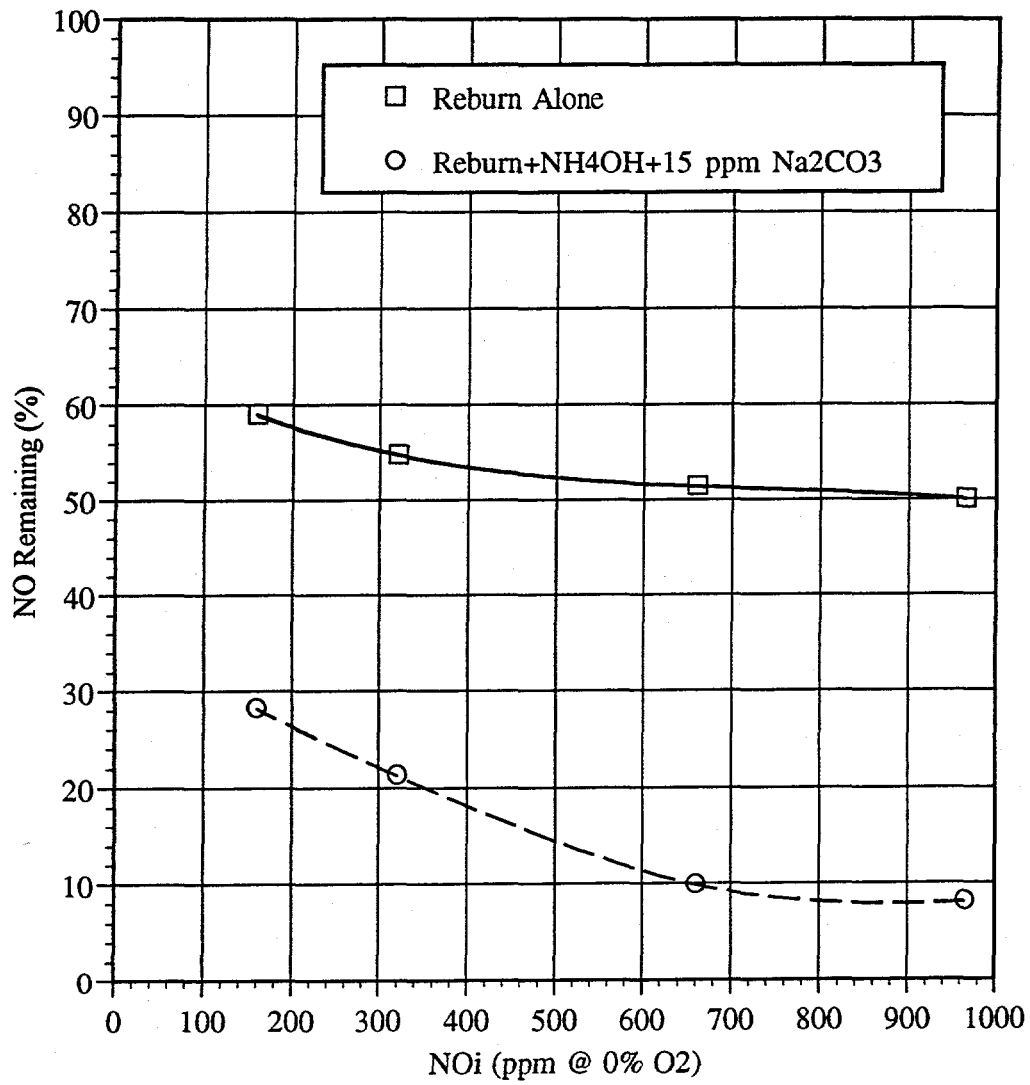


Figure 2.5.3. NO reduction vs. NOi for rich side injection of  $\text{NH}_4\text{OH} + \text{Na}_2\text{CO}_3$

Main Fuel: Natural gas @ 20 kW  
10% Reburn @ 1670 K  
OFA @ 1300 K  
Additive @ 1460 K  
SR1=1.10, SR2=0.99, SR3=1.15  
NOi=600 ppm as meas

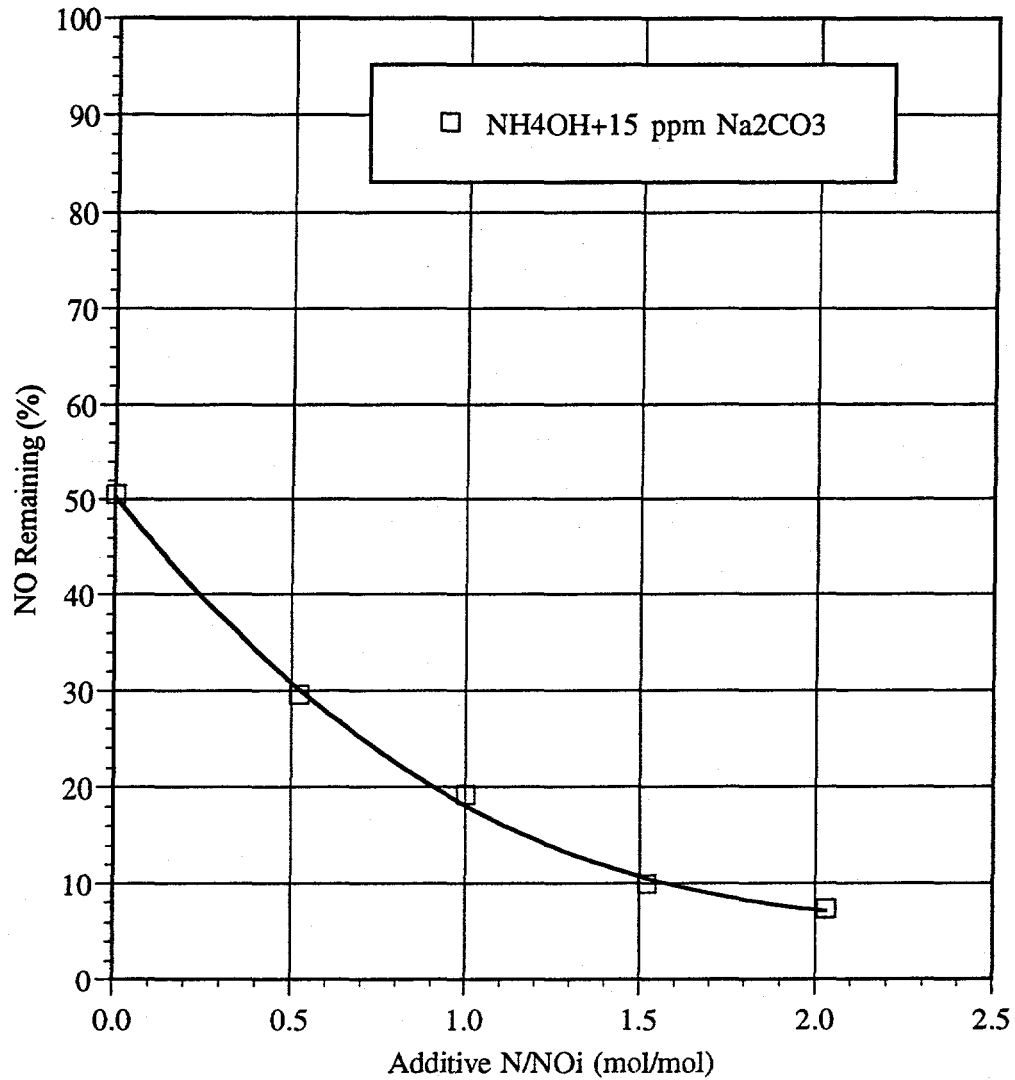


Figure 2.5.4. NO reduction vs. additive N/NOi ratio for rich side injection of  $\text{NH}_4\text{OH} + \text{Na}_2\text{CO}_3$

## 2.6 Multiple Injection Advanced Reburning

In the MIAR process nitrogen agents and promoters are injected both in the reburn zone and with the overfire air. CTT tests were conducted in which various combinations of rich and lean side additives were injected. Figure 2.6.1 shows MIAR results obtained with promoter added to the fuel rich zone. A maximum of 50% NO control was obtained by reburning alone. Advanced reburning provided up to 67% NO control. Reburning plus both rich and lean side injection of aqueous ammonia with no promoter gave a maximum of 86% NO control. The best performance was obtained with reburning with rich side injection of N-agent plus promoter and lean side injection of N-agent alone. This system reduced NO emissions by over 90%.

Figure 2.6.2 shows MIAR results obtained with promoter added to the fuel lean zone (i.e. with the overfire air). Reburning with rich side N-agent injection and lean side N-agent plus promoter injection gave up to 90% NO control. Reburning with rich side N-agent plus promoter and lean side N-agent plus promoter also provided up to 90% NO control. Moreover, these systems were largely insensitive to injection temperature, with approximately 90% NO control obtained over the entire test range of 1370 to 1590 K.

## 2.7 Bench Scale Combustion Tests: Conclusions

The 20 kW combustion tests on different variants of the AR technology make it possible to conclude that:

1. Reburning alone can achieve 50-60% NO reduction at  $SR_2=0.99-0.9$  and high temperature injection of OFA.
2. The promoted AR-Lean process demonstrates about 86% NO removal at 10% reburning and only 15 ppm  $Na_2CO_3$  in flue gas.
3. The promoted AR-Rich process is capable of removing 88% NO at 10% reburning and only 15 ppm  $Na_2CO_3$  in flue gas.
4. The MIAR process shows 90-91% NO removal and its performance is expected to increase in a larger scale facility since the injectors will not affect the temperature profile.

Main Fuel: Natural gas @ 20 kW  
 10% Reburn @ 1670 K, OFA @ 1300 K  
 SR1=1.10, SR2=0.99, SR3=1.15  
 NO<sub>i</sub>=600 ppm as meas  
 First N-agent added in fuel rich zone: N/NO<sub>ii</sub>=1.5  
 Second N-agent added w/OFA: N/NO<sub>iii</sub>=1.5  
 Na<sub>2</sub>CO<sub>3</sub> conc. in flue gas=15 ppm

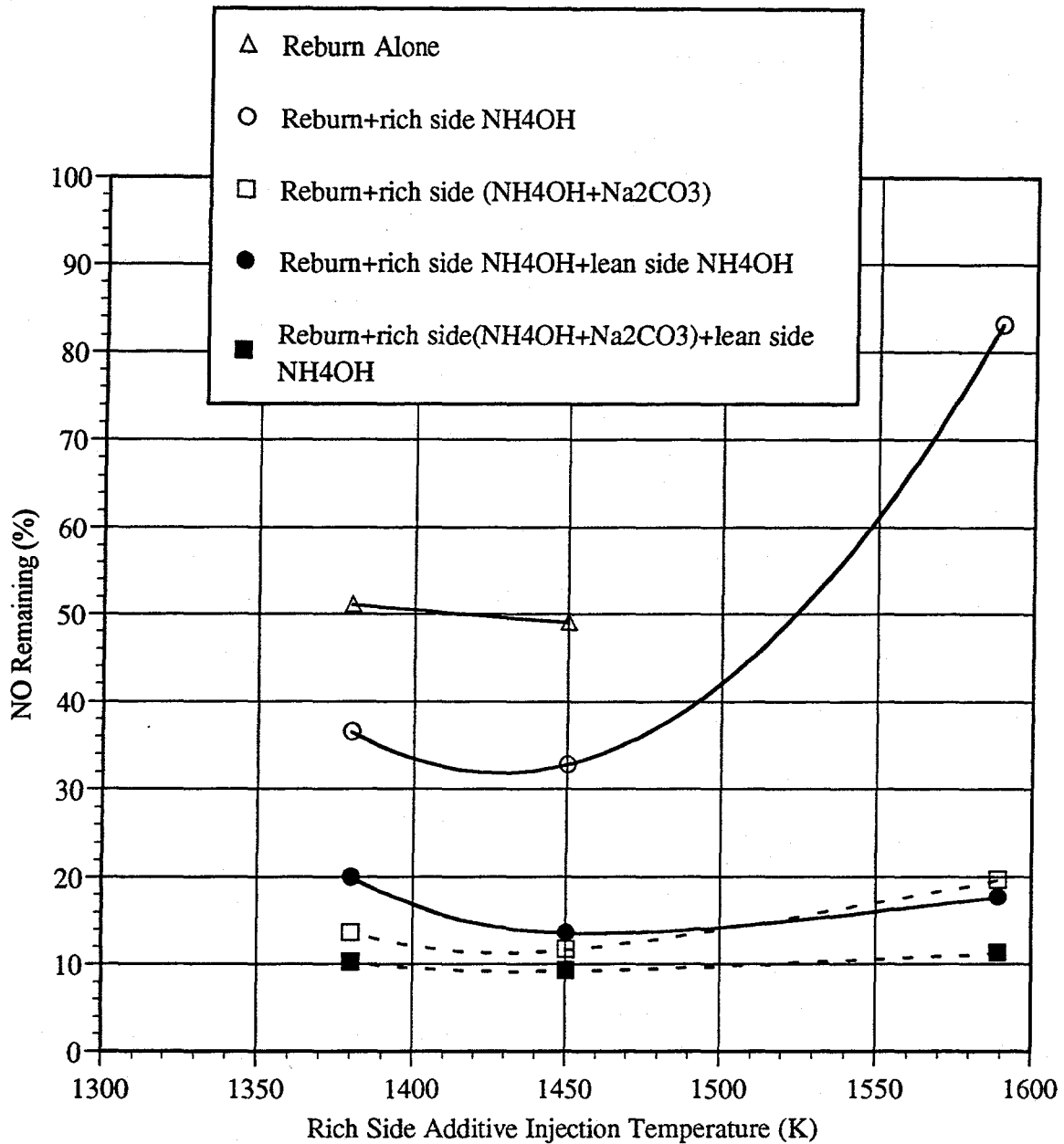


Figure 2.6.1. MIAR: NO reduction vs. additive injection temperature for reburn with both rich and lean side additives

Main Fuel: Natural gas @ 20 kW  
 10% Reburn @ 1670 K, OFA @ 1300 K  
 SR1=1.10, SR2=0.99, SR3=1.15  
 NO<sub>i</sub>=600 ppm as meas  
 First N-agent added in fuel rich zone: N/NO<sub>ii</sub>=1.5  
 Second N-agent added w/OFA: N/NO<sub>iii</sub>=1.5  
 Na<sub>2</sub>CO<sub>3</sub> conc. in flue gas=15 ppm

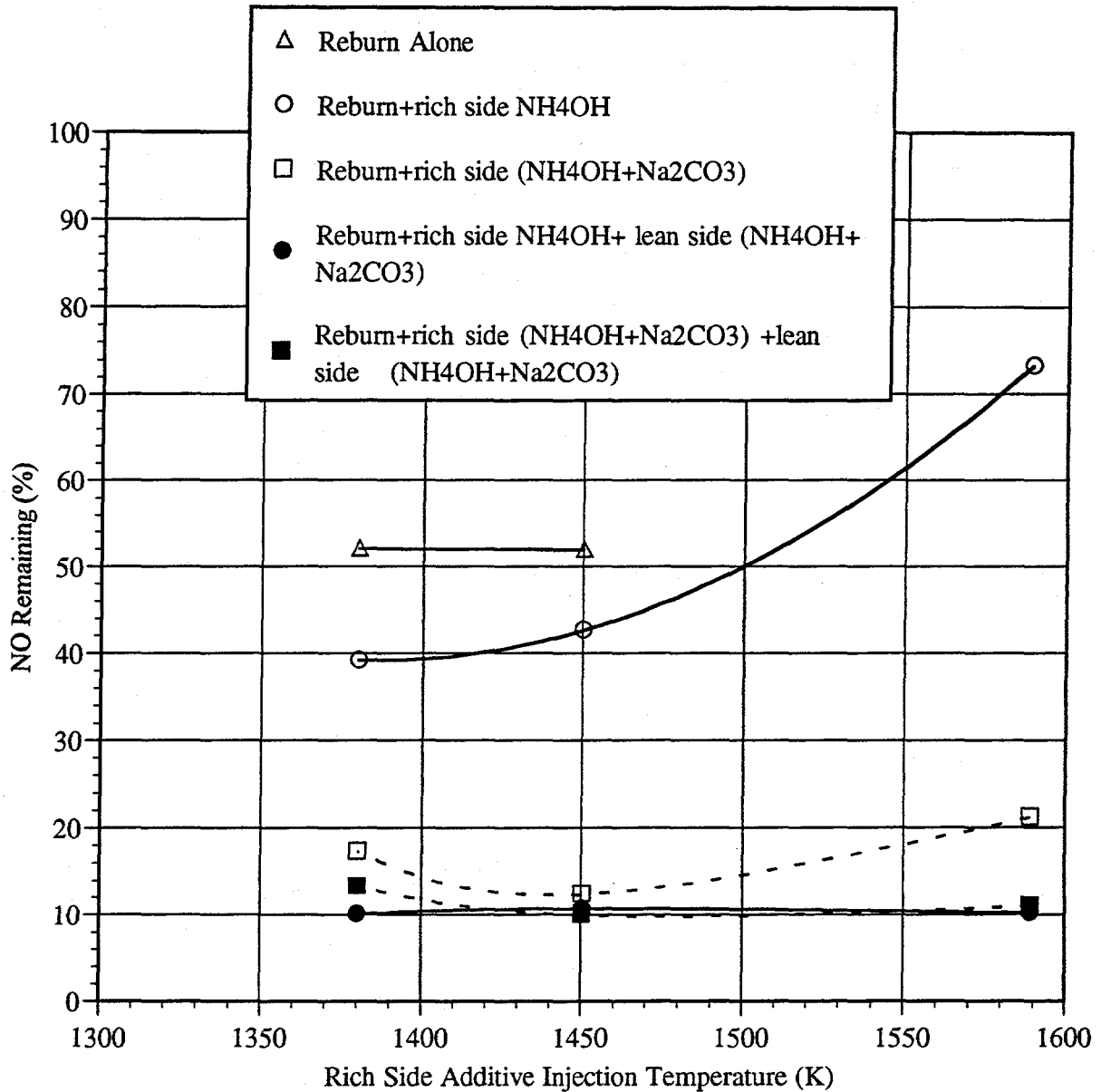


Figure 2.6.2. MIAR: NO reduction vs. additive injection temperature for reburn with both rich and lean side additives.

### 3.0 Kinetics of Sodium Reactions

Experimental and computational studies of the decomposition of sodium carbonate and other alkali metal salts, and reactions of alkali metals with components of flue gas are being conducted at the University of Texas at Austin. Section 3.0 is the Quarterly Report submitted to EER by Professor William C. Gardiner and Dr. Vitaly Lissianski.

Total direct costs expenditures for the reporting period: \$7,243.33

General Objective of the work for 4/1/96 - 6/30/96:

1. Literature review of high temperature elementary reactions relevant to addition of  $\text{Na}_2\text{CO}_3$  to flue gas.
2. Reconstruction of flow system and construction of gas handling system for gas chromatograph (GC).

During the last three months our experimental efforts were directed to reconstruction of the high-temperature flow system and to optimizing the sensitivity of our Carle GC to enable measurements of low (200 ppm) concentrations of  $\text{CO}_2$  (presumed to be the main product of  $\text{Na}_2\text{CO}_3$  decomposition) and surrogate components of flue gas. A new reactor inlet for the flow system was constructed in order to take advantage of an ultrasonic atomizing nozzle system supplied by EER.

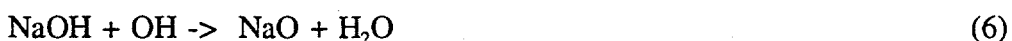
The new design includes preheating of the carrier gas to temperatures in the 300-400°C range, a ceramic adapter to isolate the nozzle system from the reactor and permit mixing hot carrier gas with spray created by the nozzle without heating the nozzle face to high temperatures. (The working temperature of the nozzle is limited to less than 200°C.) The  $\text{CO}_2$  detection sensitivity of the GC was significantly increased by cleaning, replacing thermal conductivity filaments, and a prolonged bakeout of columns at 200°C. The flow system is now operating reliably, and after calibration work is completed flow system studies of  $\text{Na}_2\text{CO}_3$  decomposition can start.

A detailed literature review on the high temperature reactions of  $\text{Na}_2\text{CO}_3$  showed that even

though salts of alkali metals have long been used as flame inhibitors (*Mitani and Nioka, 1984; Jensen and Jones, 1982*), the chemical mechanism of their decomposition and further reactions at high temperatures is poorly known. It was found that the time scale for flame inhibition is about 10 ms at 1200 K and 0.5 ms at 1800 K, which corresponds to the decomposition time of the salt (*Mitani and Nioka, 1984*). The inhibiting effect of salts was attributed (*Jensen and Jones, 1982*) to catalytic removal of H atoms and OH radicals in the chain



While Na atoms in flames have been studied for years, (*Carabetta and Kaskan, 1968; Hynes et al., 1984; Srinivasachar et al., 1990*) their reaction mechanisms are not well understood and the rate coefficients of the important reactions have not been measured. To summarize: It is known that Na, NaO, NaO<sub>2</sub>, and NaOH concentrations are coupled to one another by fast reactions which rapidly interconvert one species to another as conditions vary (*Hynes et al., 1984*). Analysis of Na influences on H<sub>2</sub>-O<sub>2</sub>-N<sub>2</sub> flames show that the Na chemistry is largely controlled by reactions:



At temperatures above 2300 K the main channel for Na disappearance is reaction (3). As temperature decreases, however, the importance of NaO<sub>2</sub> increases and the predominant depletion of sodium is via reaction (4). *Kaskan, 1971* found that reaction (4) is the dominant Na oxidation process in lean H<sub>2</sub>-O<sub>2</sub>-N<sub>2</sub> flames at temperatures from 1400 to 1700 K. Other observations also support NaO<sub>2</sub> as an important intermediate species at temperatures lower than 1900 K (*McEwan and Phillips, 1966*). However, inconsistent values of the rate coefficient for reaction (4) have been reported (*Kaskan, 1971; McEwan and Phillips, 1966; Husain and Plane, 1982*).



## 4.0 Kinetic Modeling

As described in the 2nd quarterly report (*Zamansky, 1996*), a modeling study of chemical interactions in the reburning zone had been performed. In particular, it was shown that delayed ammonia injection into the reburning zone is capable of reducing NO concentration and that certain additives, such as oxygen and active radicals, can promote the NO-NH<sub>3</sub> interaction in the reburning zone. During the current reporting period, modeling activities continued, focusing on NO-NH<sub>3</sub> interaction in the burnout zone. The following issues were addressed:

- NH<sub>3</sub> addition upstream of overfire air (OFA) injection;
- NH<sub>3</sub> co-injection with OFA;
- NH<sub>3</sub> addition downstream of OFA injection.

The CHEMKIN-II and SENKIN kinetic codes developed at the Sandia National Laboratories (*Kee et al., 1989; Lutz, et al., 1991*) were used for modeling. Calculations were performed without any adjustments in rate constants in the C-H-O-N mechanism (*Zamansky and Maly, 1996*) taking into account a BSF (Boiler Simulator Facility) temperature profile which is expected to be about 300 K/s in the reburning zone.

Modeling of the SGAR process is a multi-parametric task. SGAR includes injections of 6 different components, and each injection depends on several parameters. Injection variables and associated parameters varied in modeling are as follows:

1. Injection of the reburning fuel (CH<sub>4</sub> is considered in modeling)
  - heat input (SR<sub>2</sub>);
  - injection temperature (T<sub>1</sub>).
2. N-agent injection into the reburning zone (NH<sub>3</sub> is considered in modeling)
  - injection temperature (T<sub>2</sub>) or delay time (t<sub>1</sub>);
  - N-agent amount (A<sub>1</sub>, NSR<sub>1</sub>).
3. Promoter injection into the reburning zone
  - promoter amount (Pr<sub>1</sub>);

- mechanism of promotion.
- 4. N-agent injection into the burnout zone ( $\text{NH}_3$  is considered in modeling)
  - injection temperature ( $T_3$ ) or delay time ( $t_2$ );
  - N-agent amount ( $A_2$ ,  $\text{NSR}_2$ ).
- 5. Promoter injection into the burnout zone
  - promoter amount ( $\text{Pr}_2$ );
  - mechanism of promotion.
- 6. OFA injection
  - injection temperature ( $T_3$ ).

The chemistry which proceeds during injection modes 1-3 (reburning fuel,  $\text{NH}_3$  in the reburning zone, and rich-side promoters) was covered in the previous quarterly report (*Zamansky, 1996*). This report includes modeling of chemical interactions in the burnout zone (injection of OFA and injection of  $\text{NH}_3$  upstream, downstream and along with the OFA).

#### 4.1 Injection of Ammonia Upstream of OFA

##### 4.1.1 Effect of Oxygen

Modeling of ammonia addition into the reburning zone revealed the efficiency of the delayed  $\text{NH}_3$  injection at  $\text{SR}_2$  of about 0.99. Short delay times, about 0.1 s, relative to injection of the reburning fuel (RF) provided higher NO/TFN control efficiency. Addition of ammonia upstream of OFA is similar to delayed  $\text{NH}_3$  injection since it also results in  $\text{NH}_3$ -NO interaction under fuel-rich conditions. The delayed  $\text{NH}_3$  injection is more efficient if the delay time is relatively short, about 0.1 s, because some oxygen and active radicals still exist after interaction of the RF and the air from the main combustion zone. At longer delay times, for instance just upstream of OFA injection, there is no oxygen in the mixture and radical concentrations are very low. Therefore, injection of ammonia is inefficient. However, if ammonia is injected with small amounts of oxygen, the mixture gets a new impulse, since CO and  $\text{H}_2$  react with  $\text{O}_2$  via chain branching reactions producing radicals, which in turn participate in reactions with ammonia to form  $\text{NH}_2$  followed by the reaction of  $\text{NH}_2$  and NO.

Results of  $\text{NH}_3$ -NO interaction in the reburning zone at  $\text{SR}_2 = 0.99$  and temperatures 1500, 1400 and 1300 K are shown in Figure 4.1.1. The initial conditions accepted for calculations are the following (mixture I):

500 ppm NO - 0.16%  $\text{H}_2$  - 0.23% CO - 8%  $\text{CO}_2$  - 15%  $\text{H}_2\text{O}$  - balance  $\text{N}_2$ .

This composition in the reburning zone was found by modeling of  $\text{CH}_4$  injection with  $\text{SR}_2 = 0.99$  and 600 ppm of initial NO concentration. In 0.5 s, the NO concentration was decreased from 600 ppm to about 500 ppm and all  $\text{CH}_4$  was converted to CO and  $\text{H}_2$ .

Ammonia (500 ppm) with varied amount of oxygen are injected into mixture I. Concentrations are presented at 1 s reaction time, i.e. at 1200, 1100 and 1000 K, respectively. At these low temperatures, there is almost no change in NO and  $\text{NH}_3$  concentrations. Figure 4.1.1 is similar to Figure 2.3.2 of the previous quarterly report (*Zamansky, 1996*), results at  $T_2 = 1500$  K are shown in both figures for comparison. The NO and TFN concentrations have a clear minimum at a certain oxygen level. It is of interest that this level is higher at lower temperatures. Optimum  $\text{O}_2$  concentrations are about 100-150 ppm, 150-200 ppm, and 250-300 ppm at 1500, 1400, and 1300 K, respectively. The efficiency of NO reduction is higher at lower temperatures. At optimum oxygen concentrations, NO is reduced from 500 ppm to 100, 75, and 54 ppm at 1500, 1400, and 1300 K, respectively. The  $\text{O}_2$  concentration has a certain threshold below which NO does not react with  $\text{NH}_3$ . This threshold depends on temperature, CO/ $\text{H}_2$  concentrations, and initial NO and  $\text{NH}_3$  concentrations. At  $[\text{O}_2]$  above the optimum, the efficiency of NO removal decreases slowly. However, at  $T_2 = 1300$  K, the resulting NO concentration becomes higher than the initial one if 0.5%  $\text{O}_2$  (5000 ppm) is injected.

Thus, modeling suggests that there are two options for  $\text{NH}_3$  injection into the reburning zone: (1) immediately after the reburning fuel or upstream of OFA. In both cases, there are optimum amounts of air in the injection stream which makes it possible to efficiently decrease NO concentrations. The reduction of NO is higher at lower  $\text{NH}_3/\text{O}_2$  injection temperature.

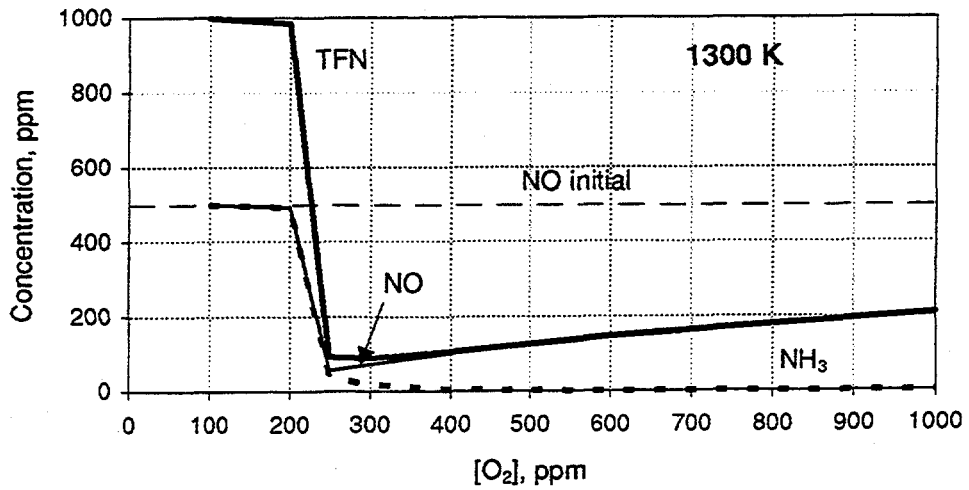
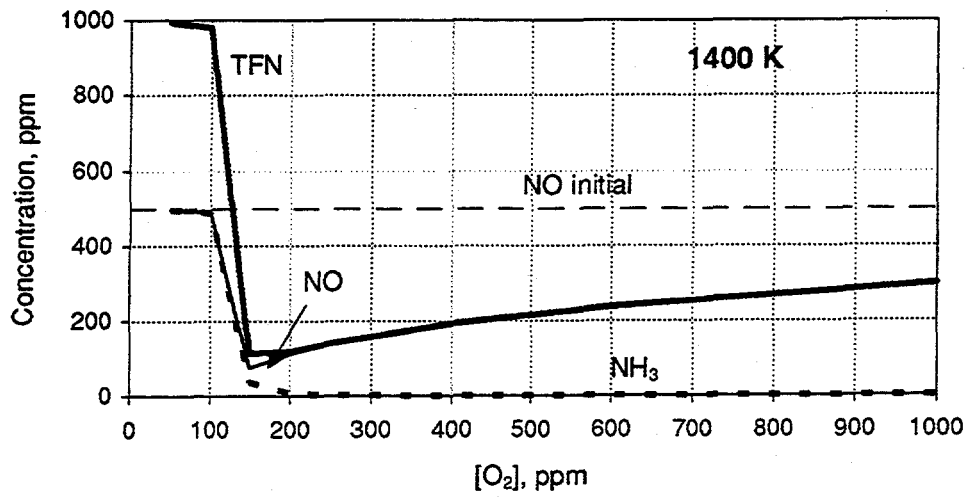
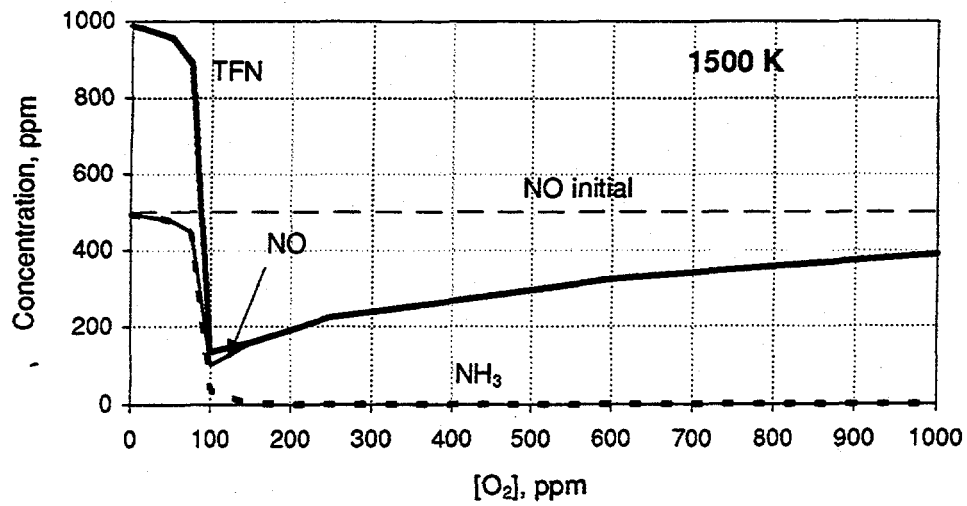


Figure 4.1.1. Effect of O<sub>2</sub> co-injection with 500 ppm NH<sub>3</sub> into mixture I at different injection temperatures.

#### 4.1.2 Effect of CO and H<sub>2</sub>

NO reduction efficiency is controlled by active radicals formed in CO and H<sub>2</sub> interaction with oxygen. Therefore, concentrations of CO and H<sub>2</sub> are important factors affecting NO-NH<sub>3</sub> interaction. The amounts of CO and H<sub>2</sub> in the mixture depend on composition of the main and reburning fuels and on the stoichiometric ratios, SR<sub>1</sub> and SR<sub>2</sub>. In all calculations SR<sub>1</sub> was 1.1. If methane is the main and reburning fuel, CO and H<sub>2</sub> concentrations depend only on SR<sub>2</sub>. Figure 4.1.2 demonstrates variation of CO and H<sub>2</sub> concentrations in mixture I (recalculated into the SR<sub>2</sub> values) with addition of 500 ppm NH<sub>3</sub> and 300 ppm O<sub>2</sub> at T<sub>2</sub> = 1300 K. Optimum conditions for NO-NH<sub>3</sub> interaction correspond to SR<sub>2</sub> = 0.99. At lower SR<sub>2</sub> values, NO reduction efficiency slightly increases, but [NH<sub>3</sub>] becomes higher as well as TFN. Under optimum conditions, NO and TFN level below 100 ppm can be achieved. Similar results were obtained for injection of 500 ppm NH<sub>3</sub> and 130 ppm O<sub>2</sub> (optimum amount) at 1500 K. The optimum SR<sub>2</sub> in that case was higher, about 0.997-0.995. Both CO and H<sub>2</sub> generate radicals in the oxidation process and help to reduce NO. The relative importance of each compound depends on conditions: temperature and concentrations of main components. For example, CO is more efficient than H<sub>2</sub> in reducing NO concentration at 1500 K, but H<sub>2</sub> has higher efficiency at 1300 K.

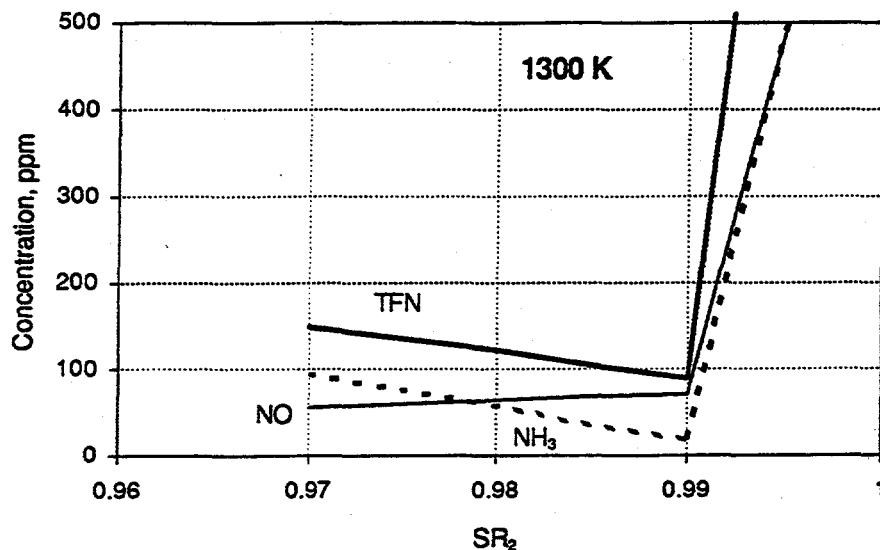


Figure 4.1.2. Effect of SR<sub>2</sub> on NO-NH<sub>3</sub> concentrations at 1300 K. 500 ppm NH<sub>3</sub> and 300 ppm O<sub>2</sub> are injected in mixture I (with variation of CO and H<sub>2</sub> concentrations).

Thus, modeling predicts that at  $T_2 = 1300-1500$  K, NO and  $\text{NH}_3$  react very slowly in the absence of CO and  $\text{H}_2$ , as well as in the absence of oxygen. NO/TFN removal is more efficient at lower temperatures with an optimum CO/ $\text{H}_2$  level in the mixture.

#### 4.1.3 Effect of Initial NO Concentration

Modeling suggests that injection of ammonia and oxygen into the reburning zone is less efficient at lower initial NO concentrations. This is demonstrated in Figure 4.1.3 which presents interaction of 200 ppm NO and 200 ppm  $\text{NH}_3$  in the reburning zone at  $\text{SR}_2 = 0.99$  and  $T_2 = 1300-1000$  K. Comparing performance at 1300 K in Figures 4.1.1 and 4.1.3, one can see that the difference in initial NO/ $\text{NH}_3$  concentrations (500 and 200 ppm, respectively) causes substantial decrease in NO removal efficiency and in the size of the window of effective  $\text{O}_2$  concentrations. At NO =  $\text{NH}_3 = 500$  ppm, TFN is reduced by more than 80%, and the process is effective in the  $\text{O}_2$  window of 250-1000 ppm. At NO =  $\text{NH}_3 = 200$  ppm, only about 50% TFN reduction is observed in the 200-400 ppm oxygen range. Figure 4.1.3 shows that a decrease in the injection temperature is capable of widening the  $\text{O}_2$  window, but the NO removal efficiency is about the same. It is worth noting that the temperatures of 1100 and 1000 K are too low and unpractical for  $\text{NH}_3/\text{O}_2$  injection upstream of OFA, since injection of OFA at too low temperatures increases unburnt amounts of CO in the mixture.

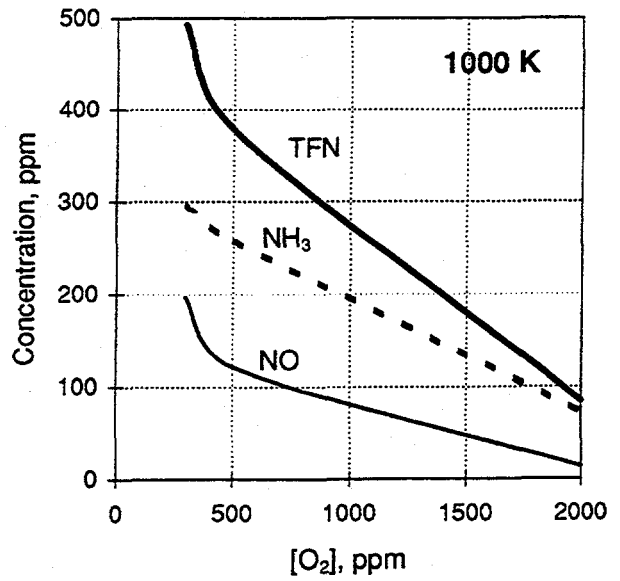
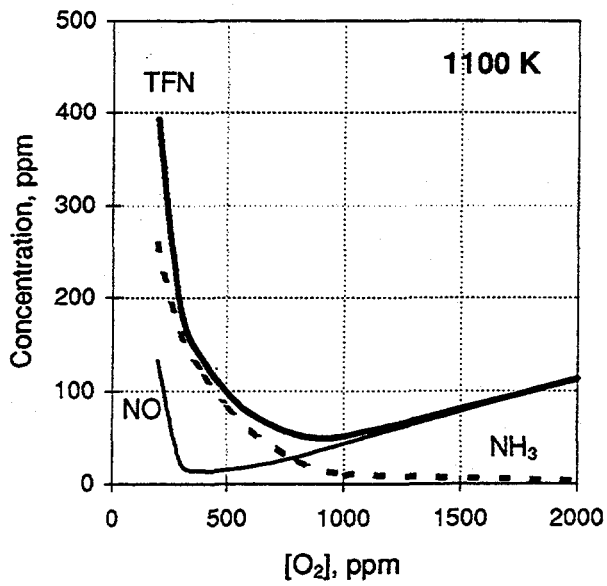
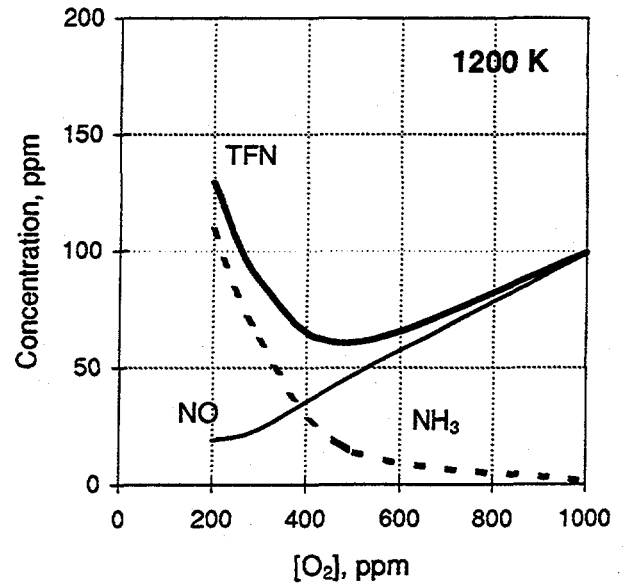
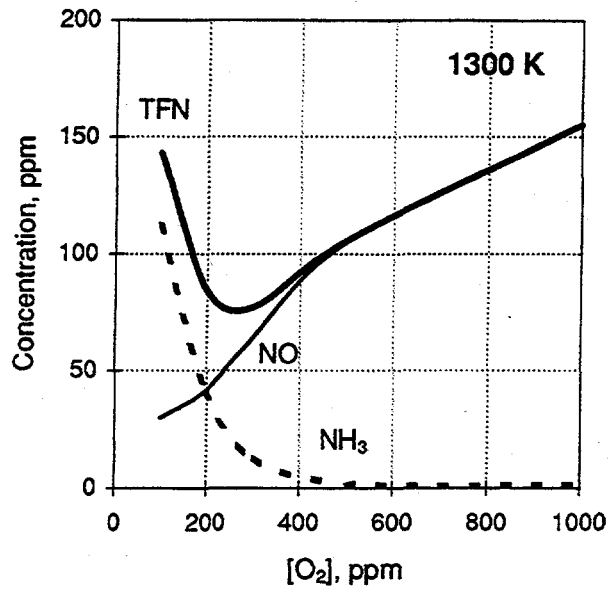


Figure 4.1.3. Temperature effect of  $O_2$  co-injection with 200 ppm  $NH_3$  into mixture I containing 200 ppm  $NO$ .

Figure 4.1.4 compares resulting NO concentrations at 1300 and 1500 K and different initial NO levels. Optimum amounts of oxygen of 130 and 300 ppm were injected at the two temperatures.

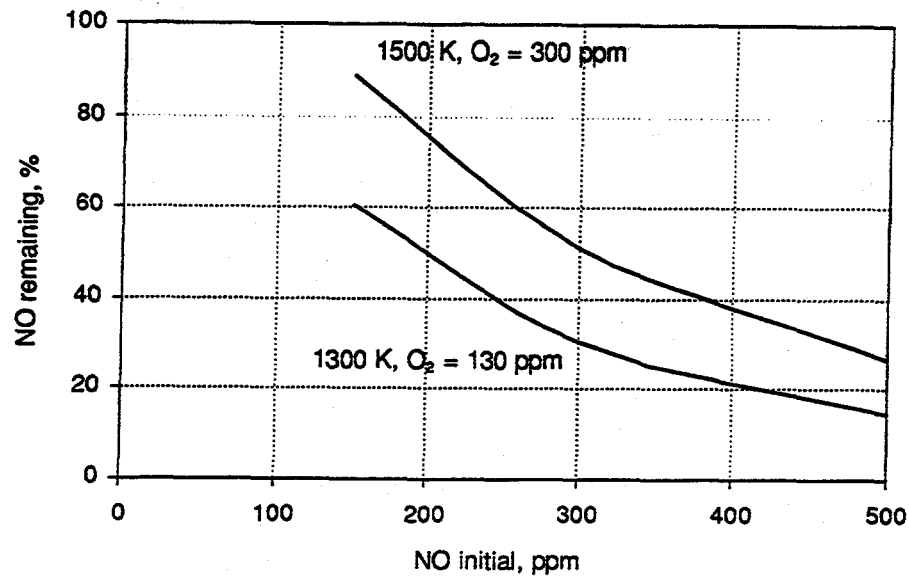


Figure 4.1.4. Effect of NO initial level on resulting NO concentration after injection of NH<sub>3</sub> (NSR<sub>1</sub> = 1.0) and the optimum amount of oxygen at 1500 and 1300 K.

#### 4.2 Injection of Ammonia with and after OFA

Modeling suggests that injection of OFA at different values of SR<sub>2</sub>, SR<sub>3</sub>, and temperature results in a final NO concentration which is near the TFN level in the mixture before OFA injection. Only at relatively high values of SR<sub>2</sub> (about 0.9) and at low OFA injection temperatures (about 1250 K), was a small decrease of final NO concentration was observed, about 15%, in comparison with the TFN concentration upstream of OFA injection.



If ammonia is injected along with OFA in the reburning zone at  $SR_2 = 0.99$ , the NO reduction process is not effective at injection temperatures above 1100 K. Figure 4.2.1 (Curve 1) demonstrates the effect of OFA injection at different locations with co-injection of ammonia at  $NSR_2 = 1.0$  on the final NO concentration. The initial NO concentration (100%, i.e. 350-500 ppm depending on the residence time in the reburning zone) increases when OFA is injected at 1120 K or higher. At these temperatures, some ammonia reacts with NO, but some is converted to NO. The resulting NO concentration ( $NO_p$ ) is higher than the initial NO concentration at the point of OFA injection ( $NO_{iii}$ ). The concentration of  $NH_3$  decreases to less than 1 ppm after the OFA/ $NH_3$  injection. Addition of higher  $NH_3$  concentration ( $NSR_2 = 1.5$ ) increases the resulting NO concentration. For instance, at  $T_3 = 1250$  K,  $NO_{iii} = 410$  ppm. Injection of 410 ppm  $NH_3$  with OFA results in 606 ppm NO, but injection of 615 ppm  $NH_3$  increases the final NO to 665 ppm. In the temperature range of 950-1050 K, the NO concentration is decreased, but this range is too low for OFA injection since all CO from the reburning zone remains unreacted.

Curve 1 represents the conditions of NO removal via the Thermal DeNOx process in the presence of high concentrations of CO and  $H_2$ . It is well known (for instance, *Lyon and Hardy, 1986*) that the presence of CO and/or  $H_2$  shifts the temperature window of NO removal by the SNCR process to lower temperatures. In order to avoid that shift, ammonia can be injected into flue gas with a short delay after injection of the OFA or in the aqueous form to allow some time for evaporation of the water. In this case, the OFA rapidly reacts with CO and  $H_2$ , and the  $NH_3$  appears in the gas mixture when all CO and  $H_2$  are already oxidized. Modeling shows that a delay time of about 0.1 s is enough for complete CO and  $H_2$  removal. The results of calculations are shown in Figure 4.2.1, Curve 2 which represents the effect of  $NH_3$  injection temperature ( $NH_3$  is injected with a 0.1 s delay time after the OFA) on NO concentrations. Under these conditions, the ammonia reacts with NO in the presence of oxygen and in the absence of CO and  $H_2$ , and the optimum temperature for  $NH_3$  injection is about 1200 K that is typical for the Thermal DeNOx process.

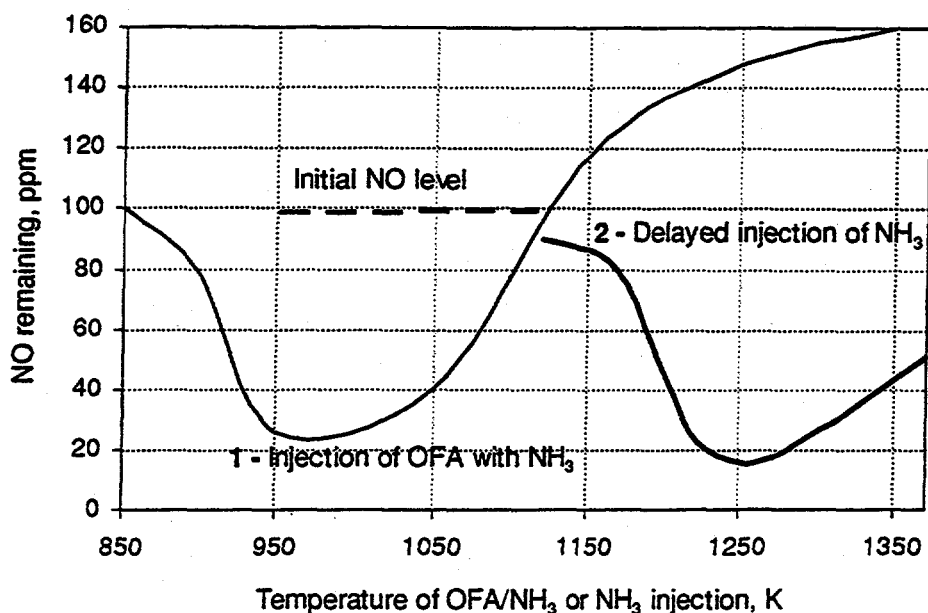


Figure 4.2.1. Effect OFA co-injection with  $\text{NH}_3$  on the final NO concentration.  $\text{NSR}_2 = 1.0$ .

If the reburning fuel is injected with  $\text{SR}_2 = 0.90$  at  $T_1 = 1700$  K, modeling shows that the concentration of ammonia in the reburning zone is higher than the NO concentration. For example, at  $T_3 = 1400$  K, concentrations of fuel-N species are the following: 71 ppm HCN, 50 ppm NO, and 113 ppm  $\text{NH}_3$ . Injection of OFA converts all fuel-N species to NO. Therefore, co-injection of gaseous ammonia with OFA does not make sense in this case either. Variation of the  $\text{O}_2$  concentration in OFA does not change the final NO level.

### 4.3 Burnout Zone Modeling: Conclusions

The modeling study on chemical behavior of ammonia in the burnout zone makes it possible to conclude that:

1. Injection of OFA into the fuel-rich reburning zone converts all fuel-nitrogen species (NO,  $\text{NH}_3$  and HCN) into NO, i.e. the TFN concentration upstream of the OFA injection nearly

equals the NO concentration downstream of OFA. At relatively high values of  $SR_2$  (about 0.9) and at low OFA injection temperatures (about 1250 K), a small decrease of final NO concentration was observed, about 15%, in comparison with the TFN concentration upstream of OFA injection.

2. Injection of ammonia with small amounts of oxygen upstream of the OFA injection location, improves NO reduction. The efficiency of NO removal depends mainly on  $SR_2$  and concentrations of oxygen, CO/H<sub>2</sub>, and NO. At  $SR_2 = 0.99$ , the optimal oxygen concentration depends on the injection temperature; it is about 100-150 ppm at 1500 K and about 250-300 ppm at 1300 K. Optimum concentrations of CO and H<sub>2</sub> correspond to  $SR_2 = 0.990$  and  $0.995$  if NH<sub>3</sub> is injected at 1300 and 1500 K, respectively. The efficiency NH<sub>3</sub>/O<sub>2</sub> injection upstream of the OFA is lower at lower NO initial concentrations.

3. Co-injection of ammonia with the OFA significantly shifts the temperature window of the Thermal DeNOx process to lower temperatures because of the CO and H<sub>2</sub> present. To avoid this shift, ammonia should be injected after a short delay time relatively to the OFA location. This delay can be provided by evaporation of aqueous ammonia or urea co-injected with OFA.

## 5.0 Future Plans

The main activities in the next quarter will include completion of the bench scale combustion experiments at the 20 kW Controlled Temperature Tower and commencement of process development tests at the pilot scale Boiler Simulator Facility. Modeling will focus on the promotion effect of sodium compounds in the burnout zone, updating the reaction mechanism to include sulfur chemistry, and sensitivity analysis to define most important elementary reactions under different conditions. Experimental program at the University of Texas on sodium kinetics under flue gas conditions will also be continued. Results will be presented at the 1996 AFRC (American Flame Research Committee) International Symposium, Baltimore, MD, September 30 - October 2, 1996.

## 6.0 References

- Carabetta, R. and Kaskan, W.E., The Oxidation of Sodium, Potassium, and Cesium in Flames, *J. Phys. Chem.* 72, 1968, pp.2483-2489.
- Husain, D. and Plane, J.M.C., Kinetic Investigation of the Reaction  $\text{Na} + \text{O}_2 + \text{M}$  by Time-Resolved Atomic Resonance Absorption Spectroscopy, *J. Chem. Soc. Faraday Trans.*, 2, 78, 1982, pp.163-178.
- Hynes, A.J., Steinberg, M. and Schofield, K., The Chemical Kinetics and Thermodynamics of Sodium Species in Oxygen-Rich Hydrogen Flames, *J. Chem. Phys.* 80, 1984, pp. 2585-2597.
- Jensen, D.E. and Jones, J.A., Kinetics of Flame Inhibition by Sodium, *J. Chem. Soc. Faraday Trans.*, 1, 78, 1982, pp. 2843-2850.
- Kaskan, W.E., The Reactions of Alkali Atoms in Lean Flames, 10th Symposium (International) on Combustion, The Combustion Institute, Pittsburgh, 1971, pp. 41-46.
- Kee, R.J., Rupley, F.M. and Miller, J.A., Chemkin-II: a Fortran Chemical Kinetics Package for the Analysis of Gas-Phase Chemical Kinetics, Sandia National Laboratories Report No. SAND89-8009, 1989.
- Lutz, A.E., Kee, R.J. and Miller, J.A., SENKIN: A Fortran Program for Predicting Homogeneous Gas Phase Chemical Kinetics with Sensitivity Analysis, Sandia National Laboratories Report No. SAND87-8248, 1991.
- Lyon, R.K. and Hardy, J.E., *Ind. Eng. Chem. Fundam.* 25, 19, 1986.
- McEwan, M.J. and Phillips, L.F., *Trans. Faraday Soc.*, 62, 1966, p. 1717.
- Mitani, T. and Nioka, T., Extinction Phenomenon of Premixed Flames with Alkali Metal Compounds, *Combust. Flame*, 55, 1984, pp.13-21.
- Srinivasachar, S., Helble, J.J., Ham, D.O. and Domazetis, G., A Kinetic Description of Vapor Phase Alkali Transformations in Combustion Systems, *Progr. Energy Combust. Sci.*, 16, 1990, pp. 303-309.
- Zamansky, V.M. and Maly, P.M., Second Generation Advanced Reburning for High Efficiency NOx Control, EER 1st Quarterly Report, DOE Contract No. DE-AC22-95PC95251, Jan. 1996.
- Zamansky, V.M., Second Generation Advanced Reburning for High Efficiency NOx Control, EER 2nd Quarterly Report, DOE Contract No. DE-AC22-95PC95251, April, 1996.